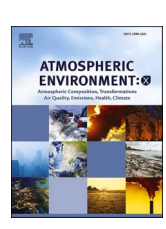
FISEVIER

Contents lists available at ScienceDirect

### Atmospheric Environment: X

journal homepage: www.journals.elsevier.com/atmospheric-environment-x



# The impact of shipping on the air quality in European port cities with a detailed analysis for Rotterdam

J.P. Tokaya <sup>a,\*</sup>, R. Kranenburg <sup>a</sup>, R.M.A. Timmermans <sup>a</sup>, P.W.H.G. Coenen <sup>a</sup>, B. Kelly <sup>a</sup>, J.S. Hullegie <sup>a</sup>, T. Megaritis <sup>b</sup>, G. Valastro <sup>b</sup>

#### ABSTRACT

Air quality in cities with large maritime ports is considerably impacted by emissions from shipping activity which is of a growing relevance due to an increasing relative contribution. To explore the extent of shipping emissions to ambient air quality, simulations with the chemical transport model LOTOS-EUROS (LOng Term Ozone Simulation – EURopean Operational Smog model) were performed for the year 2018 at an approximate  $1 \times 1$  km resolution for six European cities with large ports, i.e., Rotterdam, Antwerp, Hamburg, Amsterdam, Le Havre, and London. It was found that depending on the investigated city, 6.5%-62% of the nitrogen dioxide (NO<sub>2</sub>) concentration in the city centres is attributable to shipping activities. This corresponds to contributions of 1.8–11.5 μg/m<sup>3</sup> to the ambient air NO<sub>2</sub> concentrations. The average NO<sub>2</sub> contribution of shipping in these six cities was 28% (7.1 µg/m<sup>3</sup>). The largest relative contribution was found for Le Havre where 62% (10.8 µg/m<sup>3</sup>) of the annual average NO<sub>2</sub> concentration was caused by shipping emissions. The largest absolute contribution is found for the city centre of Hamburg with 11.5  $\mu$ g/m<sup>3</sup> (41%). The lowest absolute and relative contribution (respectively 1.8  $\mu$ g/m<sup>3</sup> and 6.5%) are found for London, also having the smallest port in terms of tonnage throughput, which is one of the influential factors that determine emission totals, investigated in this study. For the other investigated pollutants, i.e., PM<sub>2.5</sub>, PM<sub>10</sub> and SO<sub>2</sub>, contributions from shipping were less pronounced with average contribution for all cities of 10% (1.2 µg/m<sup>3</sup>) 7% (1.5 µg/m<sup>3</sup>) and 4% (0.16 µg/m<sup>3</sup>) respectively. To assess the effect of model choices on these results, this study also looked into the choice of simulation resolution and relations between meteorological parameters and NO<sub>2</sub> concentrations. Following simulations with varying chemical transport model resolutions ( $1 \times 1$  km to  $24 \times 24$  km), it is found that a decrease in ambient air pollutant concentrations away from localized emission sources is more pronounced at higher (1 × 1 km) model resolutions and source contributions are influenced more significantly than total concentrations. Considering meteorology, generally low wind speeds (1-2 m/s) lead to high NO<sub>2</sub> concentration in city centres. For the cities where the port is much closer to the city centre (e.g., London, Le Havre, Hamburg and Antwerp) the absolute NO2 concentrations as well as the contributions from shipping emissions become highest for windless conditions. The high concentrations ( $>60 \mu g/m^3 NO_2$ ) only occur when wind speeds fall below 6 m/s.

#### 1. Introduction

Elevated concentrations of air pollution cause adverse effects on human health and ecosystems. As a result of dedicated policies and legislation, emissions of air pollutants in many sectors such as energy and road traffic in Europe have decreased, leading to a declining trend for a variety of air pollutant concentrations over the last decades. In order to further reduce air pollutant concentrations the focus is being shifted to other, historically less contributing sectors, such as shipping whose relative contribution to emissions shows an increase (Brandt et al., 2013). These trends are also seen in China (Lv et al., 2018) and North America (Golbazi and Archer, 2023).

Maritime ports form a crucial part of the global freight infrastructure and maritime transport plays an essential role in the economy as one of the most energy-efficient modes of transport. It is also a large and growing source of air pollution through emissions from the combustion engines of ships and related activities in the ports. Shipping related emitted pollutant species include particulate matter (PM), nitrogen oxides (NO<sub>x</sub>) and sulphur dioxide (SO<sub>2</sub>) and can have negative impacts on human and ecosystem health by forming smog and acid rain and contribute to eutrophication (Matthias et al., 2010; Brandt et al., 2013; Jägerbrand et al., 2019; Karl et al., 2019a). Emissions from shipping can significantly affect local air quality in the vicinity of the often densely populated port areas. An overview of the effects of shipping on air quality and the impact on human health worldwide is discussed by Contini and Merico (2021). Fink et al. (2023a, 2023b) studied the impact of shipping on air pollution in the Mediterranean region by performing a multi-model comparison with a focus on PM<sub>2.5</sub> and the photo-oxidants NO<sub>2</sub> and O<sub>3</sub> respectively. Simulations with five different Chemistry Transport Models (CTMs) on a coarse resolution (12 × 12

E-mail address: janot.tokaya@tno.nl (J.P. Tokaya).

<sup>&</sup>lt;sup>a</sup> Netherlands Organization for Applied Scientific Research (TNO), Utrecht, Netherlands

<sup>&</sup>lt;sup>b</sup> Concawe, Environmental Science for European Fuel Manufacturing, Brussels, Belgium

 $<sup>^{\</sup>ast}$  Corresponding author.

km), showed that shipping emissions can contribute up to 48.1% to the  $\rm NO_2$  concentrations at several stations in the eastern part of the Mediterranean Sea where shipping lanes lie close to the shore (Fink et al., 2023b). It should be however noted that a coarse  $12\times12~\rm km$  resolution might influence the accuracy of the highly localized nature of  $\rm NO_2$  emissions. A coarse resolution relative to the localized nature of sources might lead to a smearing of the emissions as they are distributed over a larger area which reduces concentrations of peaks and generally smoothens concentrations.

Other studies (e.g. Broome et al., 2020; Tang et al., 2020) focus on a specific area domain. Ramacher et al., 2020 studied the contribution from shipping emissions to  $NO_2$  and  $PM_{2.5}$  concentrations for the city of Hamburg with an urban-scale CTM simulation on a high ( $500 \times 500$  m) resolution. With this high model resolution, it was found that emissions from shipping contributed up to 60% of the total  $NO_2$  concentrations in Hamburg at areas with a relatively high ambient air  $NO_2$  concentration (industrial and port areas). Moreover, residential areas within a distance of 5 km from the port area still experienced contributions from shipping emissions to the  $NO_2$  concentration of 20–30%.

The studies mentioned above either focus on a particular port with a high level of spatial detail or discuss multiple ports in a large region at a relatively coarse resolution. The work presented here discusses multiple ports at a high resolution in a harmonized way. Regardless of resolution, the majority of the past studies (Karl et al., 2019b; Broome et al., 2020; Ramacher et al., 2020; Fink et al., 2023) have highlighted that the contribution of shipping is of major interest to improve urban air quality and support policy making, especially in port cities. Similar results were also found in a research where the impact of shipping emissions on the air quality in Europe and 19 major port cities in Northwest Europe and the Mediterranean region (Concawe, 2023a) was studied. In that study, a  $6 \times 6$  km resolution simulation over Europe was performed and the source apportionment feature of LOTOS EUROS CTM was used to compute the contribution of shipping emissions to atmospheric air pollutant (NO2, PM10, PM2.5 and SO2) concentrations. The study showed an average contribution from shipping to the NO2 concentration over all ports of 28% with a maximum contribution of 59.5% for Bremerhaven. The study highlighted also the need for high-resolution emission inventories to improve accuracy.

The importance of emission inventories in modelling simulations has also been an objective of a similar study where high-resolution simulations were performed (approximately  $1\times 1$  km) over Northwestern Europe. It was concluded that the use of emissions at the highest available resolution should yield the best geographical resolvement of the simulated concentrations and there is a strong impact on source apportionment results. This study investigated the impact of aviation emissions on the air quality in Europe and major cities (Concawe, 2023b). Therefore, in this study the use of datasets with more detailed localization and spread of sources was recommended for source apportionment modelling.

Following the findings from the earlier Concawe study on maritime contributions (Concawe, 2023a) this paper performs a more in-depth analysis of the contribution from shipping emissions to the local urban air quality, and the importance of several impacting factors in the modelling. These factors were identified to be relevant in the aforementioned study and were further explored here. For the analysis, six cities in North-West Europe have been selected, that have a port in the top-30 largest maritime ports of Europe in terms of cargo throughput, including the four largest European ports (i.e., the ports of Rotterdam, Antwerp, Hamburg and Amsterdam). High resolution simulations (approximately  $1\times 1~\rm km$ ) were performed with the CTM LOTOS-EUROS (Manders et al., 2017). Globally three of these four ports are in the top 50 largest ports in the world (Rotterdam ranking 10th and Antwerp ranking 14th and Hamburg 43rd).

Besides the role that emission inventories and grid resolution may have on the air pollutant concentrations, meteorological conditions may also play an important role. To assess how findings are influenced by the specific meteorological conditions in the year that was investigated (i.e., 2018), relations between meteorological parameters and  $NO_2$  concentrations in the city centres were quantified.

Ambient temperature has a multitude of effects on NO2 concentrations. Firstly, there is a direct effect on emissions (e.g., higher NO<sub>x</sub> emissions due to increased residential heat demand and increased occurrence of relatively strong polluting cold start engine emissions during cold days as taken into account in the modelling through temperature dependent emission factors). Secondly, the chemical regime changes due to temperature dependent ozone formation and VOC emissions resulting in a shifting NO2:NO ratio. Precipitation also has an influence on the wet deposition of NO2 and other pollutants thereby having a direct and indirect effect on NO2 concentrations. Thirdly, there is an effect due to the changes in atmospheric dynamics as a consequence of temperature. Stable atmospheric conditions generally coincide with low temperatures and limited solar irradiation and can cause build-up of pollutants and lead to high surface concentrations. The nonlinear nature of atmospheric chemistry hampers making generalized statements on the influence of meteorological parameters on NO2 surface concentrations, but on average stable conditions (low temperature, and wind speeds) lead to high atmospheric NO2 concentrations.

In order to gain a better understanding of the aspects influencing the concentrations in the model simulations, the impact of the following factors on the modelled concentrations were analysed.

- Spatial resolution of the modelled concentrations
- Spatial distribution of the source attributed modelled concentrations.
- Meteorology
- Use of emission datasets (as analysed in Contini and Merico, 2021)

With this integral approach, the study aims to analyse how local air quality in six different port cities in western Europe are influenced by shipping emissions. Since the earlier study (Concawe, 2023a), showed that emissions from shipping have the highest contribution for NO2 concentrations (compared to other pollutants), this study mainly focusses on the effect of shipping emissions on NO2 concentrations in the selected ports/cities and only briefly discusses the other pollutants (PM2.5, PM10 and SO2) for which source attributed concentrations were modelled.

#### 2. Methods

LOTOS-EUROS is a chemical transport model (CTM) with labelling capabilities. It is used to calculate atmospheric pollutant concentrations and attribute them to underlying emission sources. This section starts with a description of the general model characteristics. This will be elaborated further with the model set-up specific to this study. The section ends with a description of the methods used to analyse and interpret model results.

#### 2.1. LOTOS-EUROS - model description and setup

LOTOS-EUROS is an Eulerian chemistry transport model (Manders et al., 2017). In this study LE v2.2.003 was used including project specific code for using high resolution emission inventories and allowing labelling of pollutants. The model simulates air pollution in the lower troposphere and is of intermediate complexity, allowing ensemble-based simulations and assimilation studies. LOTOS-EUROS performs hourly model output using ECMWF (European Centre for Medium-Range Weather Forecasts) meteorological data. The gas phase chemistry follows the TNO CBM-IV scheme (Schaap et al., 2008).

LOTOS-EUROS has a dynamical vertical layer structure that can be defined in three ways. The default option, which is used in this study, calculates directly on the layers of the meteorological model from which data was used as input (in this case ECMWF). In order to keep the

runtime within reasonable bounds, a number of layers of the meteorological model can be combined into single model layers. In this study the meteorological layers were aggregated into 12 model layers. This is the default setting in the LOTOS-EUROS model. The model will copy a level definition from the used set of meteorological data. Depending on the data this definition could define layer interfaces as pressures or heights above the surface. This method is useful to keep LOTOS-EUROS as close to a meteorological model as possible.

For the 12 model layers setting used in this study the first three layers

correspond 1-to-1 to the levels in the meteorological ECMWF input field. The fourth till 12th layer are the average of the two subsequent meteorological layers, e.g. layer four in LE is the average of layer 4 and 5 in the ECWMF data, layer 5 is the average of layer 6 and 7 in the ECWMF data and so on. The rest of the atmosphere (above the layers simulated by the model) is filled with concentrations from the global boundary conditions; these are used for top boundary conditions.

The so-called surface concentrations (reference height of 2.5 m) are calculated as output using the average concentrations in the lowest layer

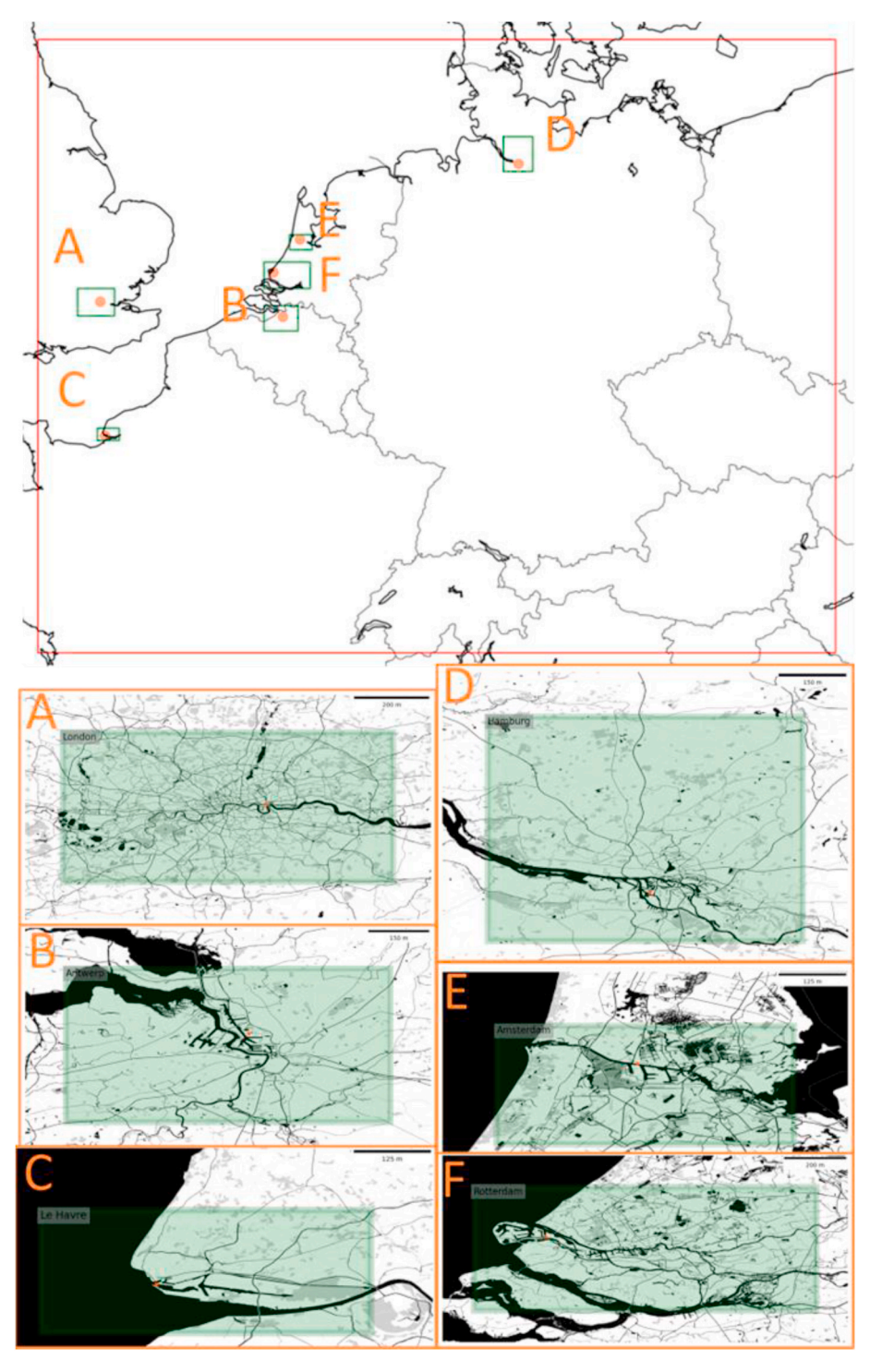


Fig. 1. Graphical representation of the domains over which the simulations are performed displaying how the high resolution simulations ( $\sim$ 1 × 1 km resolution) are embedded in the western European simulation ( $\sim$ 6 × 6 km resolution, top panel). The domains for the simulation over London, Antwerp, Le Havre Hamburg, Amsterdam and Rotterdam are shown in panels A, B, C, D, E and F respectively.

and calculating a vertical profile due to dry deposition.

The model has participated in multiple model intercomparison studies (Bessagnet et al., 2016; Colette et al., 2017), showing overall good performance with respect to other participating models.

In this study, the simulation is performed for the year 2018 and runs with a spin-up period of one week. Boundary and initial conditions are taken from the CAMS global IFS (Integrated Forecasting System) model (Rémy et al., 2022) reanalysis data.

#### 2.2. Model domains and resolutions

In order to resolve atmospheric concentration model equations at a resolution of approximately  $1\times 1$  km in the region of interest a zooming strategy was used. This means a sequence of nested simulations is performed with an increasing resolution for a decreasing domain size. An initial simulation over entire Europe (longitude range from  $-25^\circ$  to  $45^\circ$  and latitude range from  $30^\circ$  to  $72^\circ$ ) was performed at a  $0.2^\circ\times0.4^\circ$  latitude and longitude ( $\sim\!24\times24$  km) resolution. This simulation was used as a boundary condition for a simulation over western Europe (longitude range from  $-1.5^\circ$  to  $17.5^\circ$  and latitude range from  $46^\circ$  to  $55^\circ$ ) at a  $0.05^\circ\times0.1^\circ$  latitude and longitude ( $\sim\!6\times6$  km) resolution. This latter domain is displayed as a red rectangle in Fig. 1. Within this simulation six nested simulations are performed for the cities of interest at a  $1/60^\circ$  longitude by  $1/120^\circ$  latitude (approximately  $1\times1$  km) resolution.

#### 2.3. Labelling

Based on the Gridding Nomenclature For Reporting (GNFR) emissions are categorized in various sectors. Using this categorization (and its subdivision) emissions are labelled when introduced in the simulation with LOTOS-EUROS. The labelling routine is implemented for primary, inert aerosol tracers as well as for chemically active tracers containing a C, N (reduced and oxidized) or S atom, as these are conserved and traceable (Kranenburg et al., 2013).

In the simulations performed in this study, the labels used to distinguish contributions from the various anthropogenic sources are: energy, refineries, industry, residential combustion, fuel production, solvent use, road transport (with a distinction between exhaust and non-exhaust emissions), shipping (both inland and international), aviation, mobile machinery, waste, livestock, and manure management and storage. For natural sources a distinction is made between emissions from wildfires, the Saharan dessert and other biogenic sources. Lastly, concentrations entering the simulation through the edges of the domain (including from aloft) receive the label boundary.

#### 2.4. Meteorology

The LOTOS-EUROS model is run with ECMWF ERA5 reanalysis meteorological data (Hersbach et al., 2020) for the year of interest, i.e. 2018. ERA5 provides hourly estimates of a large number of atmospheric, land and oceanic climate variables, which are necessary inputs for calculating atmospheric concentrations. The ERA5 data cover the Earth on an approximate average  $30\times30\,\mathrm{km}$  grid  $(0.25^\circ\times0.25^\circ)$  and resolves the atmosphere using 137 levels from the surface up to a height of 80 km. Typical inputs required by LOTOS-EUROS are for example surface and air temperature, cloud cover, wind speed and direction, precipitation and relative humidity.

Quality-assured monthly updates of ERA5 (1959 to present) are published within 3 months of real-time and available through the Climate Data Store (CDS). Preliminary daily updates of the dataset are available to users within 5 days of real-time.

The ECMWF fields are obtained at a longitude/latitude grid, where the latitudinal spacing can be irregular. Horizontal bi-linear interpolation or area-averaging is applied to map the input to the LOTOS-EUROS (regular longitude latitude) simulation grid. The 3D fields are then mapped to the model levels using air-mass weighted averaging. In time, linear interpolation is used to obtain meteorological values at required time steps between the data frequency (3 hourly or less).

#### 2.5. Emissions

Anthropogenic land-based gridded emissions for 2018 obtained from the CAMS-REG v5.1 emission inventory (an updated version of Kuenen et al., 2022) were used as input for all simulations over Europe with a resolution coarser than  $0.05^{\circ} \times 0.1^{\circ}$  (i.e., the resolution of the emission dataset) in latitude and longitude (i.e., approximately  $6 \times 6$  km over central Europe). Gridded emission files contain GNFR emission sectors for each country for the air pollutants  $NO_x$ ,  $SO_2$ ,  $PM_{10}$ ,  $PM_{2.5}$  as well as NMVOC,  $NH_3$ , CO, and  $CH_4$ .

The distribution of emissions per sector over various heights in the model is described in Bieser et al. (2011). The temporal distribution of the annual emissions of each sector into hourly emission data with data splitting is described in Granier et al. (2019).

In the emission sets used in this study (see the overview in Table 1), the shipping emissions at sea are derived from Automatic Identification System (AIS) data of all ships sailing in the total geographic domain with the STEAM model (Jalkanen et al., 2016). These emissions are higher than the emissions reported to the European Environment Agency (EEA) as a result of the restrictive definition of maritime emissions in the national inventories of the EU Member States, which do not include any shipping emissions outside the territorial waters of the Member States. The emissions for "International maritime navigation" are defined as: "Emissions from fuels used by vessels of all flags that are engaged in international water-borne navigation. The international navigation may take place at sea, on inland lakes and waterways and in coastal waters. Includes emissions from journeys that depart in one country and arrive in a different country. Excludes consumption by fishing vessels" (EEA, 2019). These emissions (which are commonly calculated on bunker sales) cannot be attributed to a specific country as the emissions take place at sea in international waters and hence are geographically distributed using the STEAM model.

The total European  $\mathrm{NO_x}$  emissions (2018) used in this simulation were  $\sim\!9.3$  Mton for the simulation domain of which 64 kton (0.7%) originate from inland shipping and 2.2 Mton (23%) originate from international shipping emissions as reported to the EEA.

The high-resolution datasets *TNO GHG-co v1.0* (Denier van der Gon et al., 2021) and *GrETA* ((Schneider et al., 2016) and *ER* (Wever et al., 2021) are based on the CAMS-REGv5.1 dataset but have an increased resolution for particular countries or pollutants based on high-resolution proxy data or national reporting respectively. The former dataset (*TNO GHG-co v1.0*) uses proxies to best represent the spatial variability of each specific emission source such as population density, different land cover classes or a road transport network (e.g., based on open street map). The latter dataset (*GrETA and ER*) uses the Dutch national emission inventory (ER) and Gridding Emission Tool for ArcGIS (GrETA) to compute high-resolution emissions in the Netherlands and Germany.

**Table 1**Overview of the emission datasets used in the various domains.

set	Available	Remark
CAMS-REG v5.1 6 × 6 km	All locations	Coarser resolution than high- resolution simulation which results in unnatural patches in the concentration fields
TNO GHG-co 1 × 1 km v1.0 (Denier van der Gon et al., 2021)	All locations	Contains $NO_x$ , $NH_3$ , $NMVOC$ , but no data for $PM$ and $SO_2$
GrETA and ER datasets $1 \times 1 \text{ km}$	Only for locations in NL and DE. So not for London (UK), Antwerp (BE) and Le Havre (FR)	Contains $NO_x$ , $NH_3$ , $NMVOC$ , $PM$ and $SO_2$

Regarding natural emissions from sea salt, two parametrizations are used for online calculation of emissions: a) Mårtensson et al. (2003) for fine particles and b) Monahan and O'Muircheartaigh (1986) for coarse particles. Biogenic emissions are calculated online during the CTM simulation. For isoprene, a tree-species-dependent emission factor was used (Schaap et al., 2008; Beltman et al., 2013). NO emissions from soil were calculated as in Novak and Pierce (1993). There is no treatment of NO $_{\rm X}$  from lightning in LOTOS-EUROS.

#### 2.6. Model evaluation

The modelled atmospheric surface concentrations of  $NO_2$  (as well as of the other pollutants looked in this study) have been compared to measured concentrations from validated stationary air quality stations near or in the cities of interest. The measurements used for verification are collected from the Copernicus Atmospheric Monitoring Service (CAMS) dataset of surface observations, from the EEA database as well as national initiatives (e.g., a network of measurements stations in the Netherlands, called LML, i.e., Landelijk Meetnet Luchtkwaliteit or National Measurement Network on Air Quality). These networks are composed of various measurement devices for the different pollutants, but all data is quality controlled by the respective publisher.  $NO_2$  is measured with chemiluminescence (that are for example for the LML station calibrated with Palmes tubes), PM is measured with various laser

particle sensors/photo spectrometry or beta-radiation attenuation monitors and SO<sub>2</sub> generally with UV fluorescence.

The modelled and observed concentrations are compared by multiple statistical metrics. The normalized root mean square error (nRMSE) is the RMSE divided by the mean of the observations and can be interpreted as a fraction of the overall range that is typically resolved by the model. Next to this, a temporal correlation coefficient is computed to assess how well observed temporal variability in concentrations is captured by the model. Lastly, the slope of a linear regression fit of the modelled and observed concentrations is a measure of structural over- or underestimation of high or low concentrations. Ideally a 1-to-1 line is found indicating that (in combination with high correlation coefficients) the measured and modelled concentrations are well aligned. The mathematical formulations to compute the parameters of interest are as follows (overbars denote mean quantities):

Mean bias : Bias = 
$$\frac{1}{N} \sum (C_{\text{model}} - C_{\text{observation}})$$
 (1)

Root mean square error‡:

$$nRMSE = \sqrt{\sum (C_{model} - C_{observation})^2} / \overline{C_{observation}}$$
 (2)

$$Temporal \ correlation: R^2 = \left(\frac{\sum{(C_{model} \cdot \overline{C_{model}})(C_{observation} \cdot \overline{C_{observation}})}}{\sqrt{\sum{(C_{model} \cdot \overline{C_{model}})^2} \sum{(C_{observation} \cdot \overline{C_{observation}})^2}}}\right)^2$$
 (3)

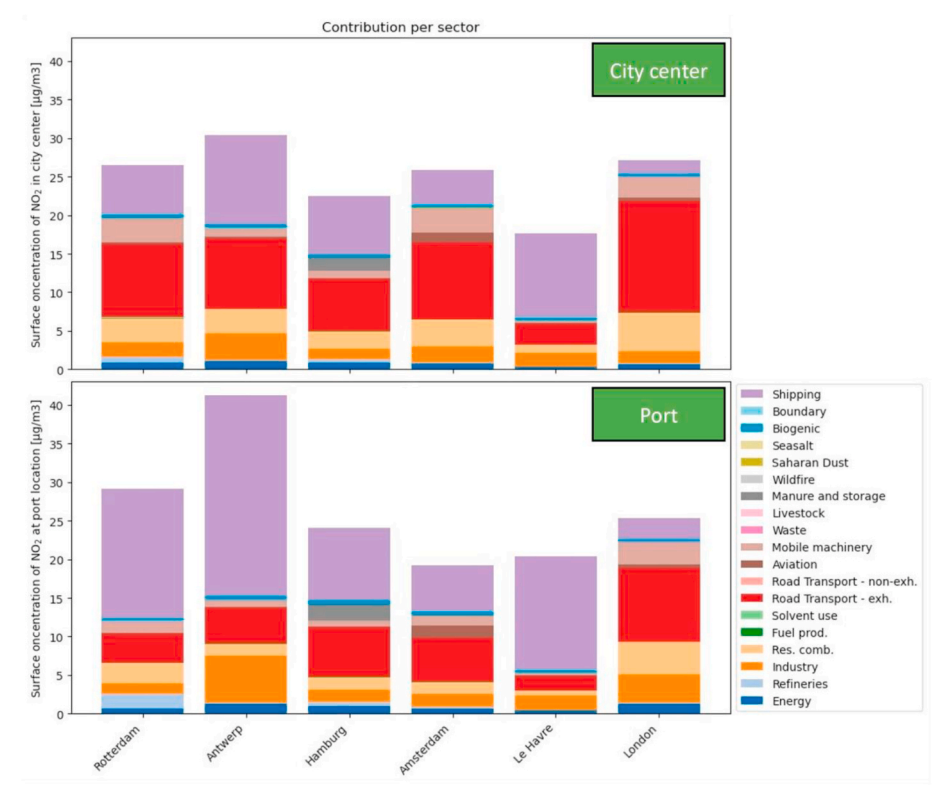


Fig. 2. The source attribution results showing the contribution from the various sectors to the annual average  $NO_2$  concentration for the six city centres and the ports. The average contribution from shipping in the chosen city centres is 28%, making this the second largest contributor after road transport exhaust emissions (35%). In the ports, the contribution to the  $NO_2$  concentration originating from shipping emissions is higher at 47%.

Table 2
Predicted annual average NO<sub>2</sub> concentration in the six city centres (top 3 rows) and ports (bottom 3 rows) and the relative contributions of the two most important contributing sectors (i.e., shipping, road transport-exhaust).

Concentration [μg/m³] (%)		Rotterdam	Antwerp	Hamburg	Amsterdam	Le Havre	London	Average
Total	City centre	26.4	30.2	22.6	25.8	17.5	27.1	24.9
Shipping		6.3 (24%)	11.5 (38%)	7.6 (34%)	4.4 (17%)	10.8 (62%)	1.8 (6.5%)	7.1 (28%)
Road Transport – exhaust		9.5 (36%)	9.1 (30%)	6.8 (30%)	10.0 (39%)	2.8 (16%)	14.4 (53%)	8.7 (35%)
Total	Port	29.0	41.2	24	19.2	20.2	25.3	26.5
Shipping		16.7 (58%)	26 (63%)	9.3 (39%)	6.0 (31%)	14.6 (72%)	2.8 (11%)	12.6 (47%)
Road Transport – exhaust		3.8 (13%)	4.6 (11%)	6.4 (27%)	5.6 (29%)	1.9 (9.4%)	9.5 (38%)	5.3 (20%)

In these equations C stands for the (modelled or observed) atmospheric concentration in  $\mu g/m^3$  and N for the total number of data points considered. The normalized RMSE (nRMSE) is the RMSE divided by  $\overline{C_{observation}}$ .

#### 3. Results

#### 3.1. Model results

The results for the cities/ports examined in the study are summarized in Fig. 2 and Table 2. For all investigated cities the air quality is moderately to significantly influenced by emissions from shipping. The lowest contribution from shipping is found for London (which also has the smallest maritime port of the six ports selected in this study), where 6.5% of the NO<sub>2</sub> concentration (adding 1.8 μg/m<sup>3</sup> to the total concentration) in the city centre (defined as the coordinates of the Big Ben) can be attributed to the shipping sector. In London, being the city with the largest population in this study, the strongest contribution (in absolute terms) to the NO<sub>2</sub> concentration is from road transport. Le Havre (where the city centre is defined as the location of l'Hôtel de Ville) on the contrary has least inhabitants and is a coastal city bordered in the north and west by the English Channel. This leads to relatively low absolute NO<sub>2</sub> concentrations which are in turn predominantly caused by shipping emissions, i.e., 62% (or 10.9 µg/m<sup>3</sup>) of the annual average NO<sub>2</sub> concentration comes from shipping. In the other cities the contribution from shipping to ambient air NO<sub>2</sub> concentrations varies between 17% (or 2.2  $\mu g/m^3$ ) (in Amsterdam at the Damplein) to 38% (or 11.5  $\mu g/m^3$ ) (in Antwerp at Onze-Lieve-Vrouwekathedraal). It should also be noted that in the ports, the shipping contribution is significantly higher than in the city centres (Table 2).

The importance of selecting a suitable location to represent the city centre is evident from Fig. 3. Since the location to represent the city centre was chosen to be within the historic and touristic city centres (e. g., the city centre of Amsterdam is represented by the Dam square, the city centre of London is represented by the Big Ben, and the city centre of Rotterdam is represented by the Beurs World Trade Centre) it is generally close to a road network. The significant contribution from road transport is clearly visible in the top panel of Fig. 3. The contribution from shipping is likewise notable for the waterways (the Rhine connecting the city of Rotterdam and the port). The exact choice of the points that represent the city centre and port strongly influence the source attribution results. It is therefore important to understand better how the contribution of the different sectors may vary spatially. For this reason, a more detailed analysis is performed for the city of Rotterdam, which is by far the largest port of Europe in terms of cargo tonnage (441 Mt in 2018).

#### 3.2. Spatial variability in $NO_2$ concentrations in Rotterdam

The simulated annual average surface concentration of  $NO_2$  around the port of Rotterdam is shown in Fig. 3. It can be seen that the emissions from shipping cause more than half of the  $NO_2$  concentration at the

location of the port (main container terminal). In the city centre the contribution from shipping is clearly reduced but still remains significant (24%).

In order to investigate further the spatial variability of the sectoral contributions, cross sectional plots (east-west and north-south) for the Rotterdam area are created and are displayed in Fig. 4. From east to west it is clear that the absolute contribution (and more drastically the relative contribution) from shipping to the local  $NO_2$  concentration increases. The source attribution results in Fig. 2 and 3 and Table 2 are therefore highly dependent on the exact locations that were selected to represent the city centre and port of interest. Next to the geographical variation in the contribution from shipping emissions, Fig. 4 shows a similar strong geographic variation for the highly localized contribution coming from road transport exhaust emissions. Similar trends are observed for the other cities (not shown).

#### 3.2.1. Temporal variability in NO<sub>2</sub> concentrations

The temporal variability in terms of daily and weekly cycles for the city centre of Rotterdam and the port are dominated by the temporal variation in a different source sector at each location, i.e., shipping for the port location and road transport for the city centre (Fig. 5). Since the emissions from shipping are introduced with a flat time profile, meaning the total annual emissions are spread evenly in time, the daily contribution from shipping to atmospheric concentrations will be dominated by boundary layer dynamics (thinner mixing layers during night time and growth of the mixing layer with increasing daytime temperature and solar surface irradiation). For road transport exhaust emissions an interplay between the aforementioned mixing layer dynamics and the temporal profile of the emissions with two rush hour peaks will influence the daily variability of the relative contribution from this sector.

The NO $_2$  concentration in the city centre of Rotterdam is highest when the wind points directly from the port to the city centre (westerly wind) or when the wind blows from the east-southeast where the traffic network is most dense (Fig. 4). The source contributions are also highly dependent on the wind direction. For example, in the port when the wind blows from the northwest the average NO $_2$  concentration of 31.2  $\mu g/m^3$  is nearly entirely (88%) caused by emissions from shipping as can be seen in Fig. 6. If the wind blows from the south-east the average NO $_2$  concentration of 38.4  $\mu g/m^3$  in the port is caused for 44% by shipping. The lowest contribution is found for northern wind. This variation is less pronounced for the city centre where shipping contributes between 14% and 49% depending on the wind direction.

It should be noted that the results shown in Fig. 6 are influenced by an average wind speed that is variable per wind direction bin (3.2 m/s for winds from the south-east to 6.2 m/s for winds from the west). Normally higher wind speeds result in lower pollutant concentrations but this is not observed for the comparatively strong winds from the west that still show a relatively high average concentration. Secondly, wind directions do not occur equally and often lead to a different number of datapoints per wind speed bin. The prevailing wind direction in Rotterdam is from the southwest (e.g., westerly wind occurred for 380 h in 2018 whereas northerly wind occurred for 149 h)

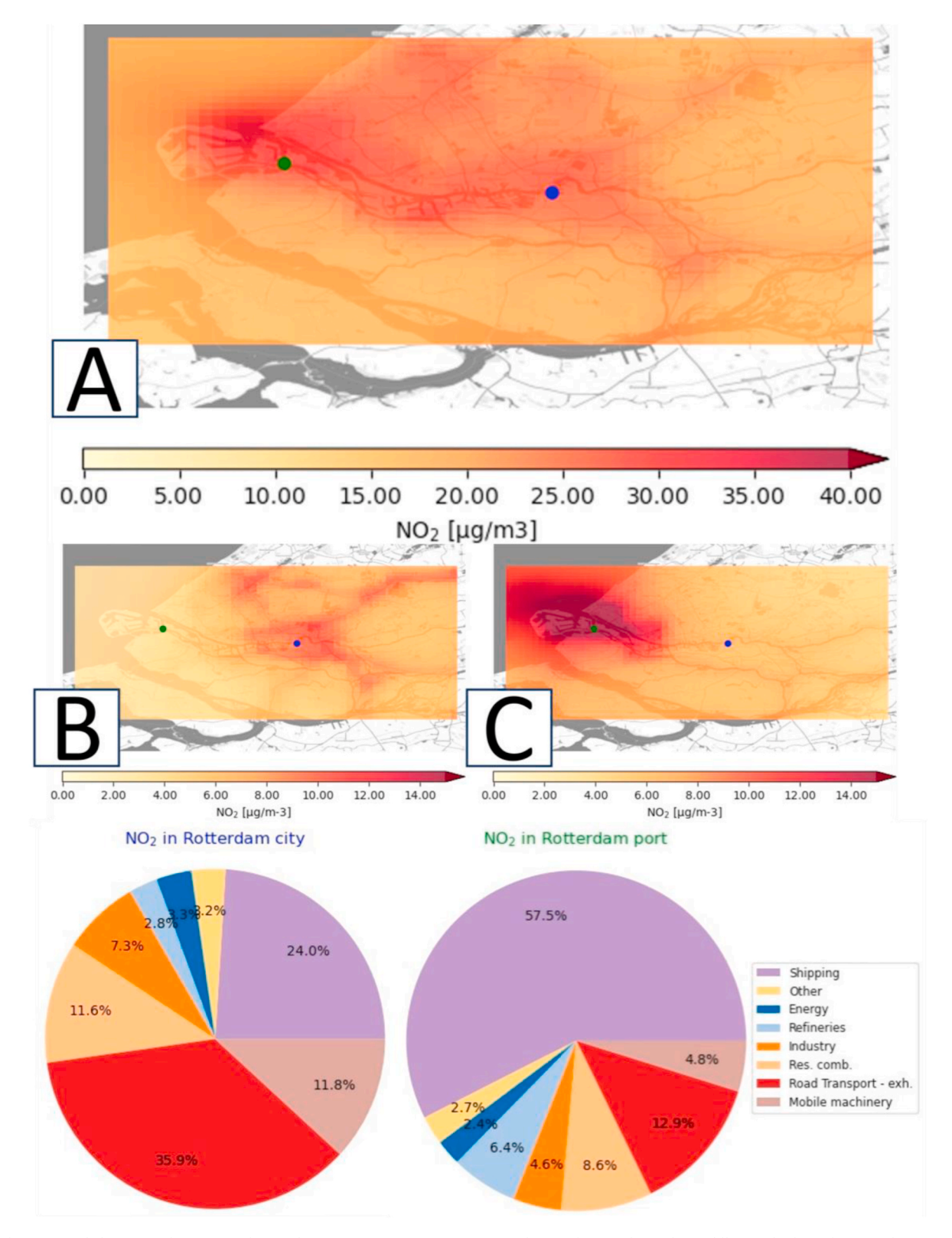


Fig. 3. The top panel shows (A) the estimated annual average  $NO_2$  concentration in and around Rotterdam. The middle panels show the annual average absolute contribution from the two most dominant sectors in the region, i.e., respectively road transport exhaust (B) and shipping (C). Yearly averaged source apportionment results for the points on the map representing the city centre (the blue dot at the location of Beursplein in Rotterdam) and main container terminal in the port (the green dot) are shown at the bottom. Results are for the  $1 \times 1$  km resolution simulation with the ER emission dataset used as input. Similar results for the other cities can be found in appendix (A). (For interpretation of the references to color in this figure legend, the reader is referred to the Web version of this article.)

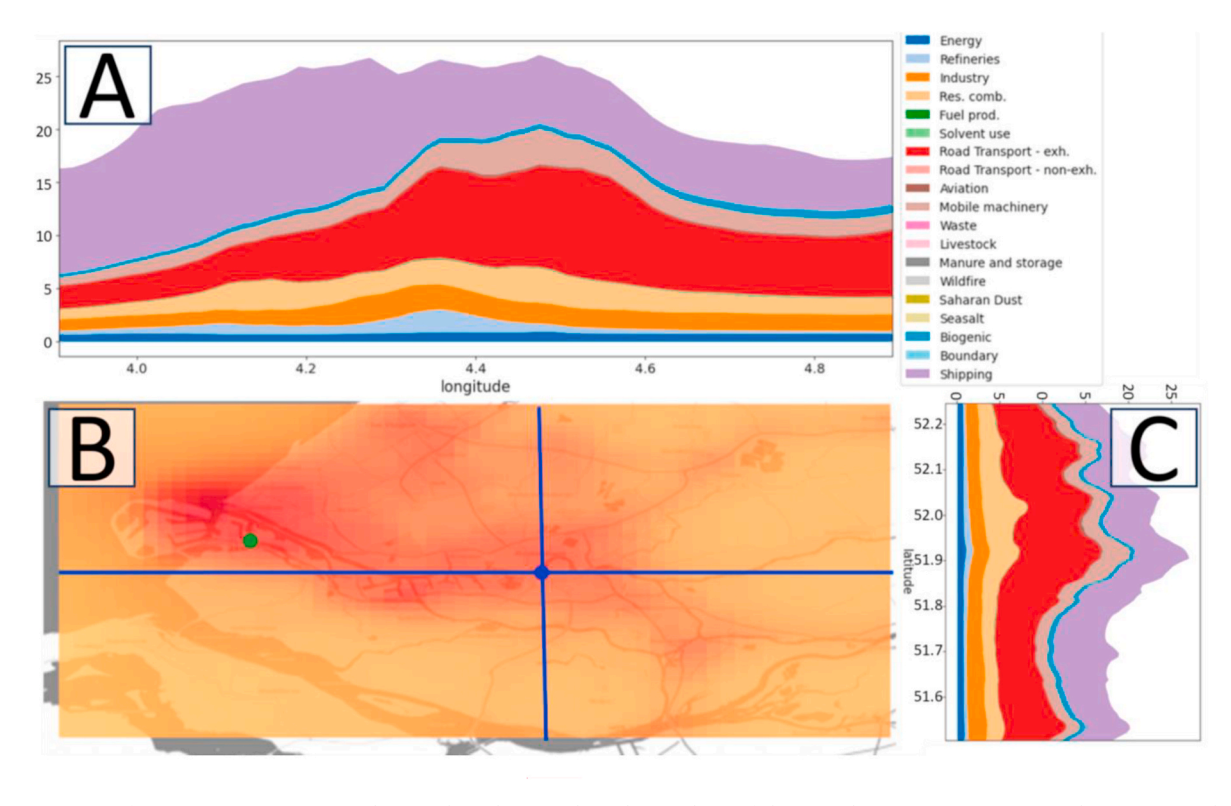


Fig. 4. Cross sections from west to east (top panel, A) and north to south (right panel, C) of the annual average concentration (shown in B) and the source apportioned contributions in the cross sections.

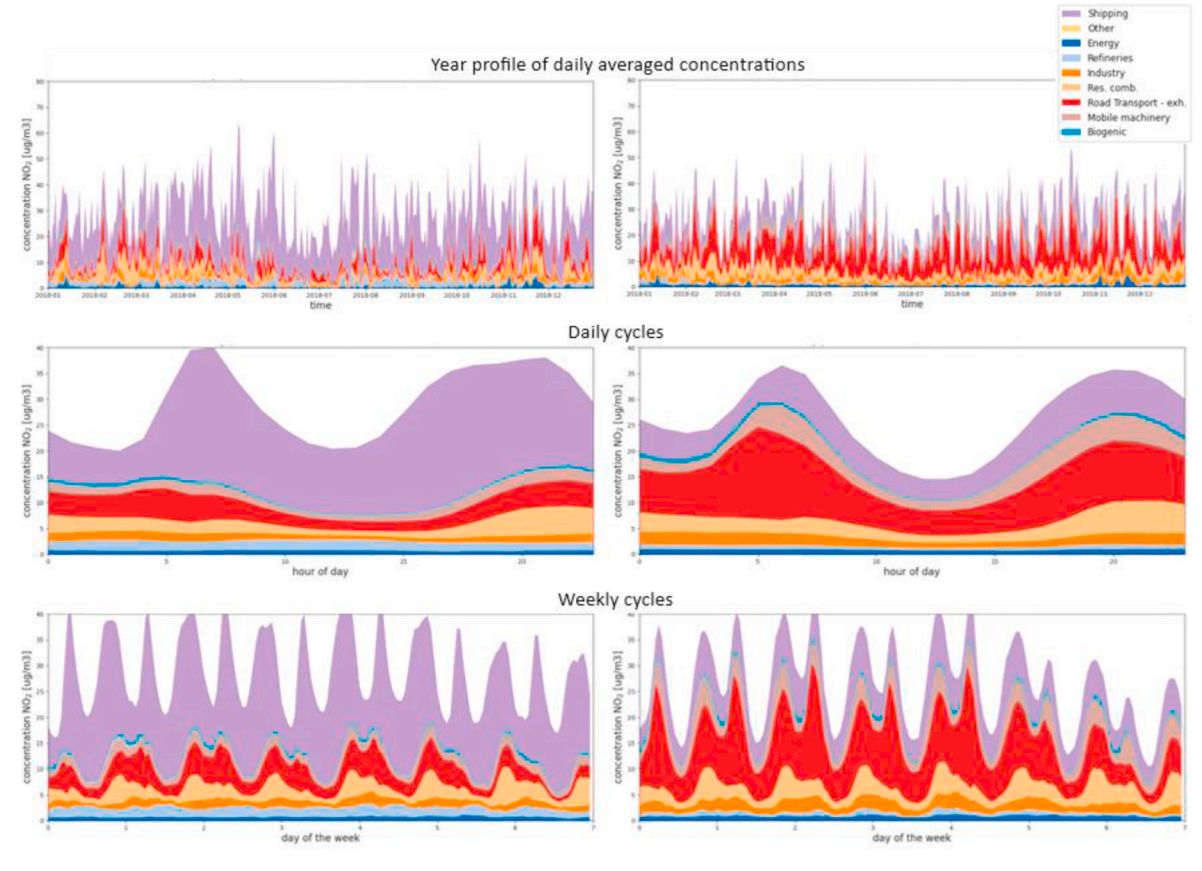


Fig. 5. Temporal variation of the  $NO_2$  concentration in the port (left) and the city centre (right) of Rotterdam.

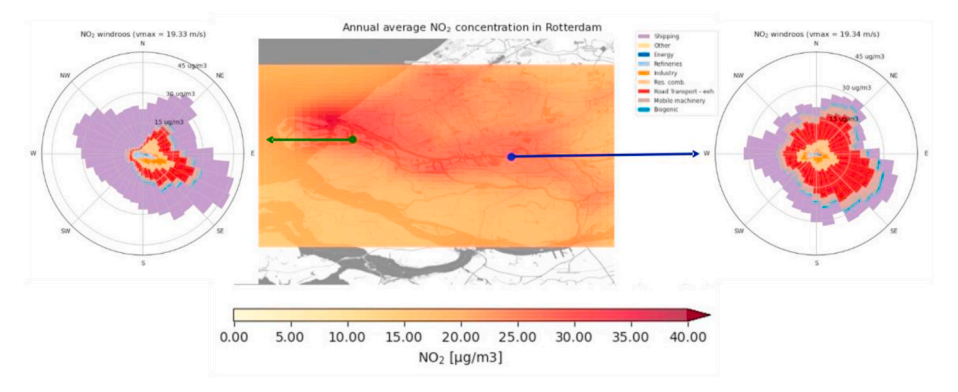


Fig. 6. Wind roses showing the average concentration for a given wind direction (bins of 10°) and the contribution from the various sectors to this concentration.

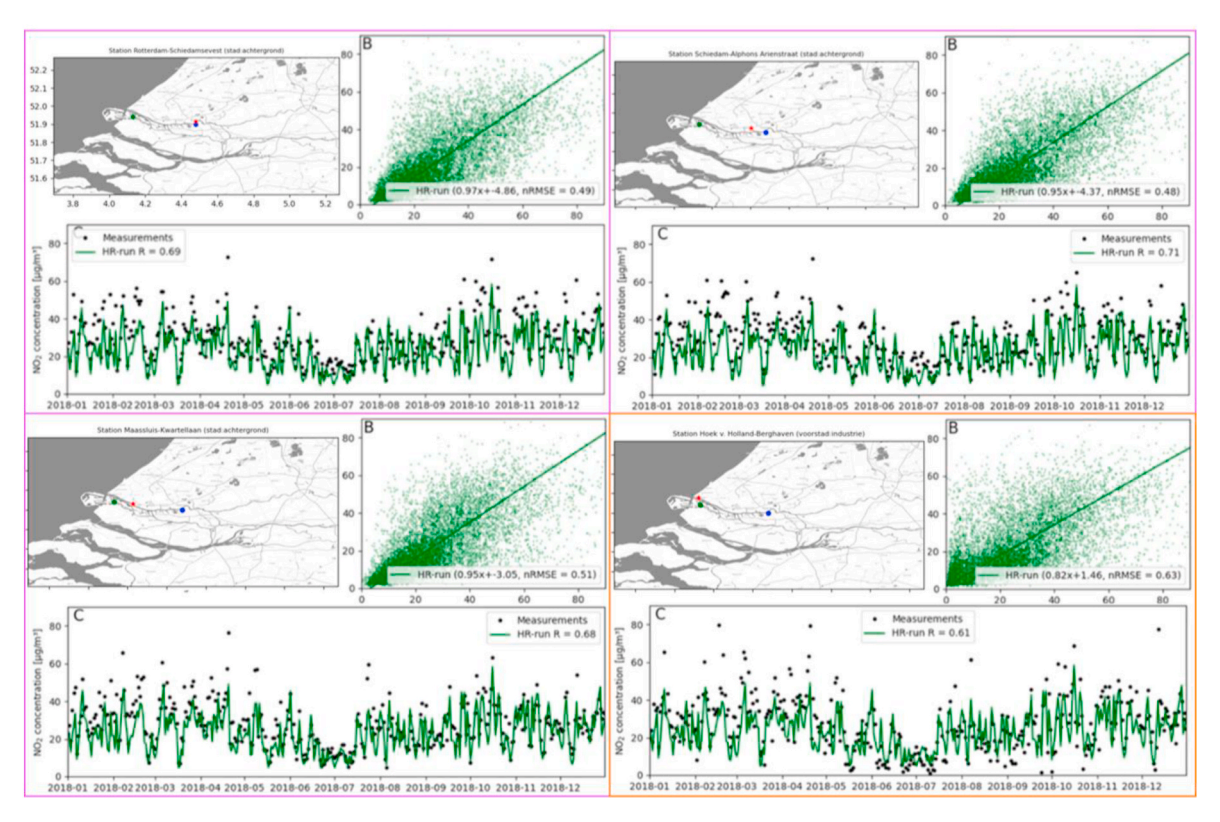


Fig. 7. Comparison between measured NO<sub>2</sub> hourly concentration in the simulation domain close to the Rhine and the modelled equivalents. Three urban background stations in Rotterdam (purple frames) and a sub-urban site in an industrial area (orange frame) were selected for the comparison. These sites are part of the LML network (Luchtmeetnet.nl, last accessed 2023–04). Subpanels A show the location of the selected measurement station (red dots). Panels B show the scatter plot of hourly averaged NO<sub>2</sub> concentrations observed by the measurement station versus the simulation results. Panels C show the underlying daily averaged time profiles. The measurements are displayed as black dots. (For interpretation of the references to color in this figure legend, the reader is referred to the Web version of this article.)

#### 3.3. Model performance

The LOTOS-EUROS modelled air pollutant concentrations in Rotterdam have been evaluated through comparison with monitoring stations observations. Hourly averaged NO $_2$  concentrations are monitored and reported structurally by the LML. Linear interpolation of the model data to the four measurement site locations enables comparison of model outcomes with measured concentrations. Given the model resolution of  $1\times 1$  km, the model results are most representative for (urban) background locations. Observations from locations classified as industrial or traffic are expected to give higher and more rapidly varying concentrations than the model. Therefore, mainly urban background stations have been selected for the evaluation. From the four selected

sites in the Rotterdam area shown in Fig. 7 it is clear that the hourly concentrations are captured reasonably well by the model even though the highest measured concentrations are not seen in the model results. The model is able to reproduce the temporal variations in the concentrations well which is reflected in moderate to good correlations for the four stations (R ranging between 0.61 and 0.71). The fitted linear regressions are fairly close to the 1-to-1 line (slope coefficient ranging between 0.82 and 0.97). The biases range from 3.5  $\mu$ g/m³ (Hoek van Holland) to 5.9  $\mu$ g/m³ (Schiedam). It should be noted that the correlation and nRMSE is found to be weakest for the sub-urban site located in an industrial area (orange frame), potentially due to misrepresentation of actual industrial emissions in the generic time profiles used to model them as well as uncertainties in the total emissions.

For the other pollutants the agreement of modelled daily average concentrations with measurements was checked in a similar way. For  $SO_2$  the performance was relatively poor (for the 4 measurement stations closest to Rotterdam the average correlation  $R^2=0.11$  and  $SO_2$  concentrations tend to be underestimated a factor of 2–3). For  $PM_{2.5}$  and  $PM_{10}$  the agreement was similar to (actually slightly worse than) the agreement seen for  $NO_2$  (for  $PM_{2.5}$  the average correlations is 0.64 and for  $PM_{10}$  is 0.61). This is also in line with performance seen for LOTOS-EUROS in other projects (Timmermans et al., 2022). Generally  $SO_2$  is notoriously challenging for LOTOS-EUROS to model accurately, but likewise challenging to measure. An important missing  $SO_2$  source in LOTOS-EUROS are from volcanic emissions which are not taken into account.

#### 4. Main factors influencing the model results

Various factors will influence the effect that shipping has on local air quality in the model results. Clearly, not all of these factors are physically significant but rather an effect of the performed analysis or simulation. This section aims to explore the variability in the shipping contribution to the  $\rm NO_2$  concentration due to these factors as well as variability due to physical processes. It will be discussed what relative changes are observed due to for example meteorological conditions and how these compare to changes caused by model resolution or emissions inventory.

#### 4.1. Model resolution

The disaggregation of emissions to higher spatial resolution as well as the added detail in the modelled chemical and transport processes will influence the predicted pollutants concentrations as it is shown in Fig. 8. In this figure, results for the city centre of Rotterdam are shown for three different model resolutions (i.e.,  $24\times24$  km,  $6\times6$  km and  $1\times1$  km). The simulations are performed with identical emission datasets (ER). The annual average  $NO_2$  concentrations at the city centre location in the middle ( $6\times6$  km) and highest ( $1\times1$  km) resolution model runs are 13% and 7% higher respectively than in the coarsest ( $24\times24$  km) resolution. The resolution also influences the source apportionment

results. The change in the source apportionment results at the Rotterdam city centre location is more pronounced than the respective change in the absolute concentration results, with a decrease of over 35% in the absolute contribution to NO<sub>2</sub> from shipping (from 9.9  $\mu$ g/m<sup>3</sup> to 6.3  $\mu$ g/ m<sup>3</sup>) and an increase of the road transport exhaust contribution of more than 40% (6.7  $\mu$ g/m<sup>3</sup> to 9.5  $\mu$ g/m<sup>3</sup>) for the highest resolution model run relative to the coarsest model run. Nonetheless, the shipping contribution remains significant since even at the highest resolution it causes nearly a quarter of the NO2 concentration in the city centre. These differences in the contributions can be explained by the fact that the highresolution simulation provides a result which is more representative for the exact location near traffic sources, while the coarse model run provides an average over a large area, including also locations where there is less traffic. This means that the decrease in concentration enhancement away from a highly localized sources will be less strong at a coarser resolution leading to a lower but more spread-out contribution. This is also the reason that the NO2 concentration in the city centre is lower for the 1  $\times$  1 km resolution relative to the 6  $\times$  6 km resolution because emissions from the ring road and neighbouring highways are on average moved away from the city centre in the highest resolution simulation.

It should be noted that in principle at a higher resolution a more detailed meteorological dataset could be beneficial. All simulations used ERA5 fields as input (on a 31 km grid) and hence the meteorological fields are not resolved at more detail with the increasing resolution, despite the fact that possibly exist for the simulations at  $6\times 6$  km and  $1\times 1$  km resolution. The land use information (which is available at a 100 m resolution) that was input, including the orography, does benefit from the improved resolution as well as the lifetime of the various chemical constituents of the atmosphere due to a more detailed modelling of high concentrations near strong emission sources.

#### 4.2. Meteorological conditions

Fig. 9 shows the hourly  $NO_2$  concentration in the city centre plotted against various meteorological conditions for the year 2018, i.e., wind speed, wind direction, ambient temperature and precipitation. These points are color-coded based on the month of the year they occurred to highlight when certain conditions occurred. The solid and dashed lines

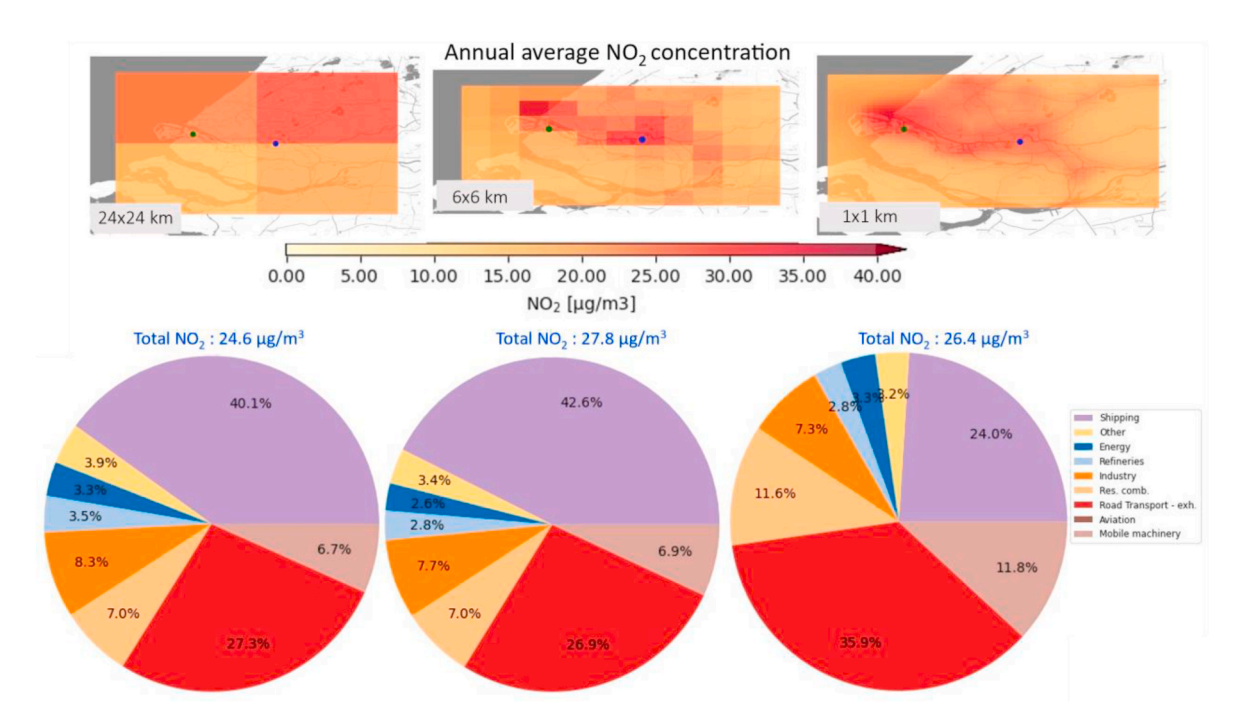


Fig. 8. The annual average NO<sub>2</sub> concentration over Rotterdam for the simulations at the various resolutions and the source apportionment results in the city centre (blue dot). (For interpretation of the references to color in this figure legend, the reader is referred to the Web version of this article.)

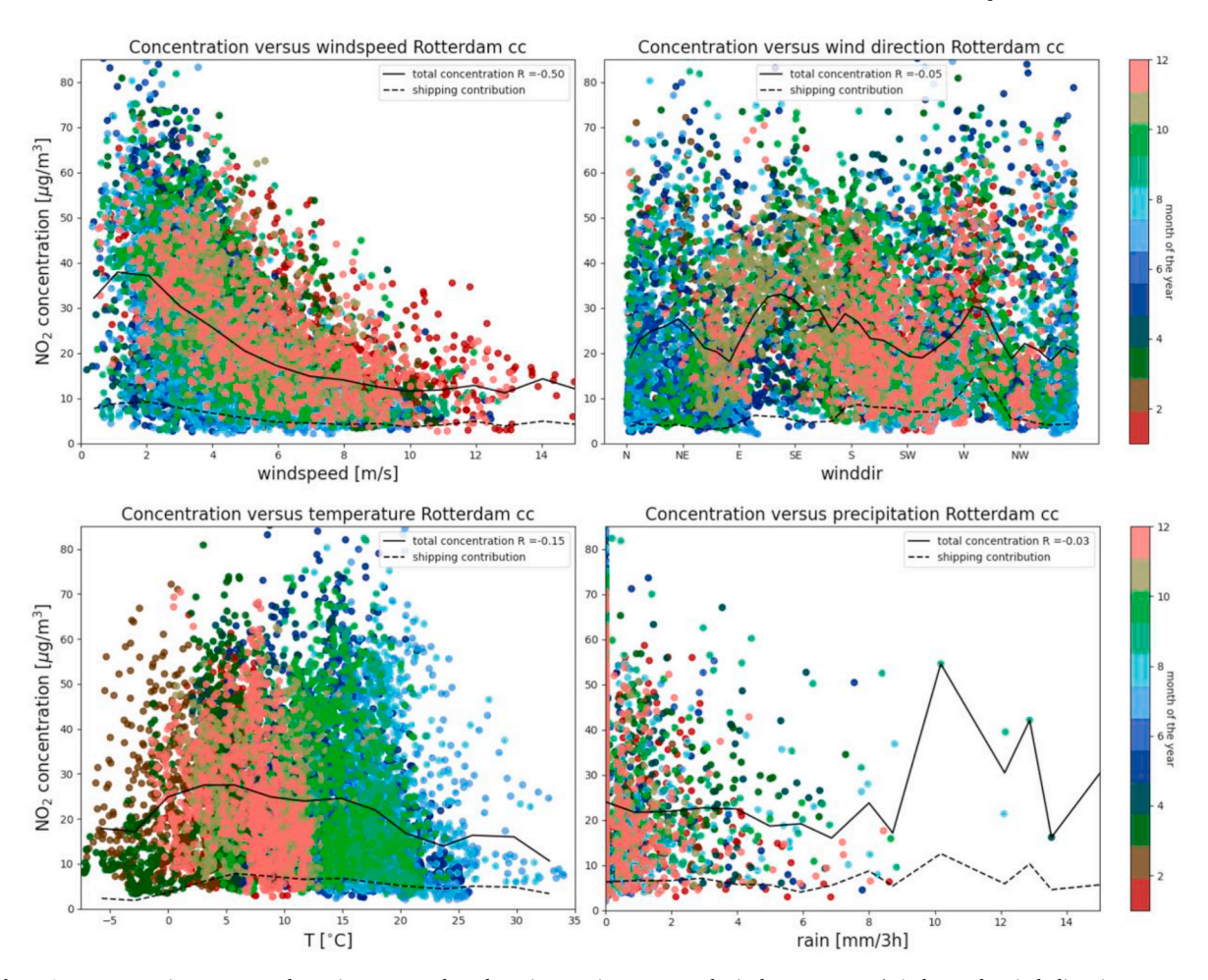


Fig. 9. The NO<sub>2</sub> concentration at Rotterdam city centre plotted against various meteorological parameters (wind speed, wind direction, temperature and precipitation).

in the figures show the average total and shipping attributed  $\rm NO_2$  concentration during specific meteorological conditions. These curves show the average  $\rm NO_2$  concentration for wind speeds discretized in 1 m/s bins, the wind direction in 10-degree bins, the precipitation in 1 mm/3 h bins and temperature in 3  $^{\circ}\text{C}$  bins.

The wind conditions strongly influence the contribution that shipping emissions have on the NO2 concentration in cities. If the wind is directed from the port to the city centre logically high NO2 concentrations caused by shipping occur as can be seen for Rotterdam in Fig. 6. Next to the direction, the wind speed also influences the concentration. Generally, extreme wind conditions lead to lower NO<sub>2</sub> in cities as higher wind speeds lead to more transport and more dilution. However, for the case of Rotterdam, the city centre is around 35 km away from the port and in windless conditions pollution from the port will hardly influence the air quality in the city centre. For each location there will be an 'optimal' wind direction and speed which transports most emissions from the port to the city centre dependent on the distance between port and city, and the lifetime of the pollutant of interest. These can be deduced from Fig. 9. The wind direction and speed that result in the highest average NO2 contribution from shipping are west-north-west with a speed of 1-2 m/s. This corresponds to a maximum transport directed from the port to the city centre. Higher wind speeds lead to more dilution (and increased mixing) and lower speeds will not transport NO<sub>2</sub> to the city centre fast enough with respect to the lifetime of the pollutant.

From the bottom left plot in Fig. 9 it appears that the highest  $NO_2$  concentrations occur when the temperatures are between -3 and 15 °C, which is a broad range. Caution has to be taken with this notion because

temperature is correlated with solar radiation intensity that causes photochemical production of ozone and hence indirectly influences  $\rm NO_2$  concentrations next to the direct effect through temperature induced boundary layer changes. From the bottom right plot in Fig. 9 it appears that high precipitation rates coincide with high NO $_2$  concentrations, but this conclusion is not statistically sound because of the low occurrences of precipitation rates  $> 8~\rm mm/3~h.$ 

It can furthermore be seen that hourly  $NO_2$  concentrations vary between 5 and  $80~\mu\text{g/m}^3$  for all wind directions. The high concentrations (>60  $\mu\text{g/m}^3$ ) only occur when wind speeds fall below 6 m/s which mainly happens when temperatures are between 10 and 15 °C.

## 4.3. Location of the port with respect to the city centre and selected receptor region

The distance of the main container terminal, where most of the shipping activity takes place, to the city centre strongly effects the severity of the air quality deterioration caused by shipping. For the various investigated ports, the distance between the city centre and the port varies between 35 km for Rotterdam and cities where the port is adjacent (within 10 km) to the city centre (Le Havre, Antwerp, Hamburg and London). For these cities windless conditions will lead to the highest concentration as well as the highest contribution from shipping. The fact that London still shows a relatively small contribution from shipping emissions to the  $\rm NO_2$  concertation is caused by the fact that the port is the smallest port in terms of tonnage throughput (e.g., 8 times smaller than Rotterdam) and the position of the city centre relative to the port.

Next to the distance between the port and the city centre, the

The drop-off of the shipping contribution to the NO<sub>2</sub>concentration

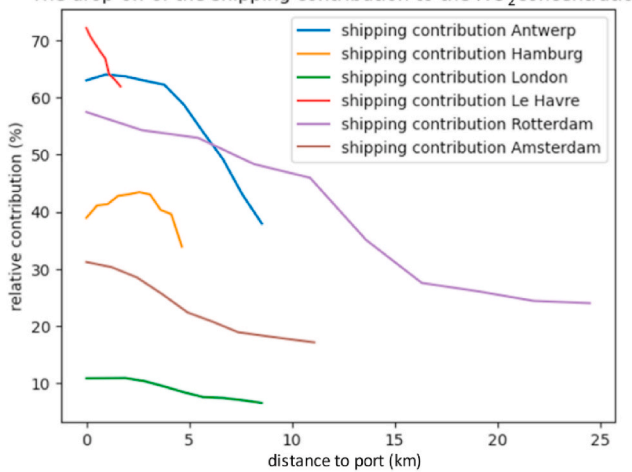


Fig. 10. The drop-off in relative contribution from shipping emissions to the  $NO_2$  concentration in the six investigated ports as a function of distance to the port. The distance between port location and what is denoted as city centre (end point of the curve) drastically differs for the six cities.

selection of the source receptor region (a point of interest aimed at reflecting the city centre) is strongly influencing source apportionment results as can be seen in Fig. 4. The significance of selecting a representative location becomes more pronounced when the resolution of the simulation increases. The added detailing in the emission input makes it more important if a point selected for representing the city centre is incidentally located for example in the vicinity of a busy road or a strong point source.

Also, the wind direction for 'optimal' transport of shipping emissions towards the city centre, similar to the top right graph in Fig. 9, is determined (completely) by the wind direction from the port location towards the point chosen to represent the city centre.

Fig. 10 shows that with increasing distance from the port (toward the city centre) a decrease in the relative contribution from shipping to the  $NO_2$  concentration is observed. It is however noteworthy that the dropoff rate is different for the different ports. It seems that the highest dropoff rate is seen for Le Havre (which also has the highest relative contribution). This trend seems to hold for most of the ports. The ports with the highest relative contributions show the fastest drop-off rates with increasing distance from the port.

#### 5. Discussion

The CAMS-REG and TNO GHG-co emission inventories that are used as input to LOTOS-EUROS are prepared using national emission data as reported in the Informative Inventory Reports of all EU member states (Kuenen et al., 2022). These reports are published annually and scrutinised during annual EU reviews. However, one should bear in mind that these inventories (by agreed definition) do not hold (geographically referenced) emission figures for international shipping in international waters. For example, if a ship travels overseas from one port to another in the same country, the emissions can be subscribed to that counties' national emissions. However, when a ship is travelling overseas from one country to another it is unclear to which country the emissions should be allocated. To analyse the international shipping emissions, the international shipping emissions are calculated by the STEAM model (Jalkanen et al., 2016) for 2018 and (spatially distributed) incorporated into the CAMS-REG emission inventory. These calculations cover all shipping emissions in the EU (seas), hence also those not included in the national inventories. These independently calculated shipping emissions using the STEAM model define the required spatially distributed seagoing shipping emission input to the LOTOS-EUROS model. The

spatial disaggregation of the shipping emissions is based on vessel AIS signals and the temporal disaggregation is based on the assumption that international shipping is a continuous activity, meaning a flat time profile is used.

In order to construct the CAMS-REG emissions inventory, the spatially distributed emissions from all other sectors in the individual Member States are also included in the dataset. Large point sources as reported to the European Environmental Agency are included in the database at the exact point source location.

The level of detail of the spatially distributed emissions will affect the outcome of the model run. It is expected that when improving the resolution of the emissions, it will increase the accuracy of the calculated air pollutant concentrations, when the model resolution also increases. Also improving the temporal distribution of the emissions through the use of local information and activity data is expected to improve the representation in the model.

The comparison between measured NO<sub>2</sub> hourly concentrations and model results have a moderate to good temporal correlation (Fig. 7). For the emissions, generic time profiles are used, e.g., continuous shipping emission at a constant rate, whereas real-world emissions have less predictable temporal variability. This difference in emission timing will result in decreased correlations. Secondly, measuring NO<sub>2</sub> accurately is not trivial. In the LML network for example (https://www.rivm. nl/bibliotheek/rapporten/680705020.pdf), uncertainties in measured concentrations of 20–25% are reported. Thirdly, the representativity of measurement data is limited to locations and times while contributions from localized sources are limited or diluted because of the model resolution of  $\sim 1 \times 1$  km. For example, a plume from a chimney that in reality can be highly localized will be diluted over the  $1 \times 1$  km grid cell in the modelled concentration, leading to lower concentrations in the model than the real measurement.

An overview was made throughout this study to describe the effect of shipping in or near cities with a large maritime port on the local air quality. This was done by computing the concentration of several air pollutants emitted by shipping. The results in this work were focussed on NO2 but the pollutants SO2 and PM have also been modelled. For conciseness we focussed on the largest port in Europe, i.e., Rotterdam, but similar analyses were performed for the other selected port cities. However, the other pollutants (PM, SO<sub>2</sub>) show a different picture. For PM the highest concentration in Rotterdam occurs when the wind direction is east south-east and wind speeds are low. Similar observations can be made for all 6 port-cities in the study. This has to do with the fact that local sources (in particular residential combustion) in the city centre are responsible for a substantial fraction of the PM<sub>2.5</sub> and PM<sub>10</sub> mass (16% and 9% for the six cities on average respectively). For SO<sub>2</sub>, similar wind conditions (direction and speed) as found for NO2 cause the highest concentrations in the city centre of Rotterdam. This is because the main source contribution comes from industry and many industrial sources are located in or near the port. On average for the six port-cities in this study the largest contribution of  $SO_2$  comes from industry (38%).

An import pollutant which has not been considered in this study, is ultra-fine particles (UFPs), i.e., particulate matter with a diameter smaller than  $0.1~\mu m$ . These are also emitted by exhausts from ships (Alanen et al., 2020; Kuittinen et al., 2021). Currently, no adequate regulations or ambient air measurement network exist for this size class of atmospheric particulates, which hardly contribute mass to the regulated PM<sub>10</sub> and PM<sub>2.5</sub> concentrations. In theory, UFPs contribute to both PM<sub>10</sub> and PM<sub>2.5</sub> but due to their small size when expressing air pollution in  $\mu g/m^3$  they hardly contribute to total mass (a particle with a diameter of 2.5 µm weighs about the same as 16 billion particles with equal density of 0.1 µm). However, these ultrafine particles are believed to have more aggressive health implications than those classes of larger particles (Howard, 2009). In modelling UFPs, not the mass but the particle number is of interest. In this study, this type of air pollution has not been taken into account even though more than 50% of UFPs in the Rijnmond area near Rotterdam for example have been shown to originate from shipping emissions (Visschedijk and Denier van der Gon, 2022).

#### 6. Conclusion

Shipping emissions contribute significantly to atmospheric pollutant concentrations in areas around large maritime ports and port cities. For example, in the Rijnmond region around Rotterdam almost 30% of the NO2 annual average concentration in 2018 originated from a combination of international and inland shipping emissions. The results for other cities show that the shipping contribution to air NO2 in the nearby city centres can even exceed 60%, but on average add 28%. Similar relative contributions are found for other European cities with large ports, where in some cases the contribution of shipping emissions is shown to be dominant compared to other sectors such as road transport. For the six port cities examined in this study, the relative contribution from international shipping to the NO2 concentration in the city centre was 28% on average (year 2018), making this sector the second largest contributor (after road transport exhaust emissions). The significance of emissions from shipping on the air quality in cities around large ports in Europe indicates that mitigation policies aimed at reducing emissions from shipping can be effective for improving the air quality in large port-

In order to investigate local effects a high-resolution simulation is required to avoid the smearing of emissions over larger areas. Moving from 24  $\times$  24 to 6  $\times$  6 and 1  $\times$  1 km resolution can drastically alter the simulated pollutant concentrations, the geographical distributions and most significantly the source apportionment results. The highest maximal concentrations in the domain are found at the highest resolution, but not all locations show an increase in concentration. For the city centre of Rotterdam, it was observed that increasing the resolution from 24  $\times$  24 to 6  $\times$  6 km leads to an increase of 13% in the NO  $_2$  concentration in the city centre, because the emissions from the city are more localized. Increasing the resolution further (to 1  $\times$  1 km) leads to a subsequent reduction of 5% of the NO2 concentration because the Rotterdam ring road emissions no longer occur in the grid cells the city centre is composed off. Next to these changes in total pollutant concentration, the source attribution results show an even more clear variation with respect to model resolution. For the city centre of Rotterdam, the highest resolution model run shows a decrease of the absolute contribution to NO2 from shipping of over 35% (offset by an increase of the road transport exhaust contribution of more than 40%) relative to the coarsest model run. For source apportionment studies, the high resolution is required to accurately distribute localized emissions from point sources, emissions from traffic on the road network or shipping on the water ways.

Another model choice that is determining levels of modelled concentrations to a large extent is the used emission dataset. In this study three state-of-the-art emission datasets were tested and a selection was made based on the resolution and completeness of these emission datasets. The datasets  $\it TNO~GHG$ - $\it Co~v1.0$  and  $\it GrETA$  and  $\it ER$  have high resolution  $\it NO_{\rm X}$  emission data for the ports of interest. The former does not contain high resolution  $\it PM$  emissions and is used for Antwerp, Le Havre and London. The  $\it GrETA$  and  $\it ER$  datasets use the Dutch national

emission inventory (ER) and Gridding Emission Tool for ArcGIS (GrETA) to compute high-resolution emissions in the Netherlands and Germany and are used for Amsterdam, Rotterdam and Hamburg.

Next to these model choices natural conditions influence ambient air pollutant concentrations. The wind conditions strongly influence the contribution that shipping emissions have on the NO2 concentration in cities. Under specific wind conditions the relative contribution from shipping emissions will be highest. For the port of Rotterdam, the wind direction and speed that result in the highest average contribution from shipping are west-north-west and 1-2 m/s respectively. For the cities where the port is much closer to the city centre (e.g., London, Le Havre, Hamburg and Antwerp) the concentrations become highest for windless conditions. It can furthermore be seen that hourly NO2 concentrations vary between 5 and 80 µg/m<sup>3</sup> for all wind directions for the city centre of Rotterdam. This is also observed for the other cities, i.e., the full range of NO2 concentration values occur for all wind directions. The high concentrations (>60  $\mu$ g/m<sup>3</sup>) only occur when wind speeds fall below 6 m/s and mainly happen when temperatures are between 10 and 15  $^{\circ}$ C. The fact that relatively low wind speeds lead to high NO<sub>2</sub> concentrations is a generality for all investigated cities and applies also to other air pollutants and is a consequence of minimal pollutant dispersion and atmospheric dilution in high emissions zones (like the investigated city

Shipping impacts the air quality in cities with large ports, mainly in terms of  $NO_2$  concentrations but also significantly in terms of PM concentrations. To determine the fractional contribution from shipping high resolutions simulation are required with up to date and high resolution emission data.

#### CRediT authorship contribution statement

J.P. Tokaya: Writing – review & editing, Writing – original draft, Formal analysis, Data curation. R. Kranenburg: Software, Methodology, Conceptualization. R.M.A. Timmermans: Writing – review & editing, Validation, Supervision. P.W.H.G. Coenen: Writing – review & editing, Supervision, Project administration. B. Kelly: Data curation, Conceptualization. J.S. Hullegie: Project administration, Methodology, Funding acquisition. T. Megaritis: Writing – review & editing, Writing – original draft, Validation, Resources, Methodology, Investigation. G. Valastro: Writing – review & editing, Writing – original draft, Supervision, Resources, Project administration.

#### **Declaration of competing interest**

The authors declare the following financial interests/personal relationships which may be considered as potential competing interests:

TNO reports financial support was provided by Concawe. If there are other authors, they declare that they have no known competing financial interests or personal relationships that could have appeared to influence the work reported in this paper.

#### Data availability

Data will be made available on request.

#### Appendix A

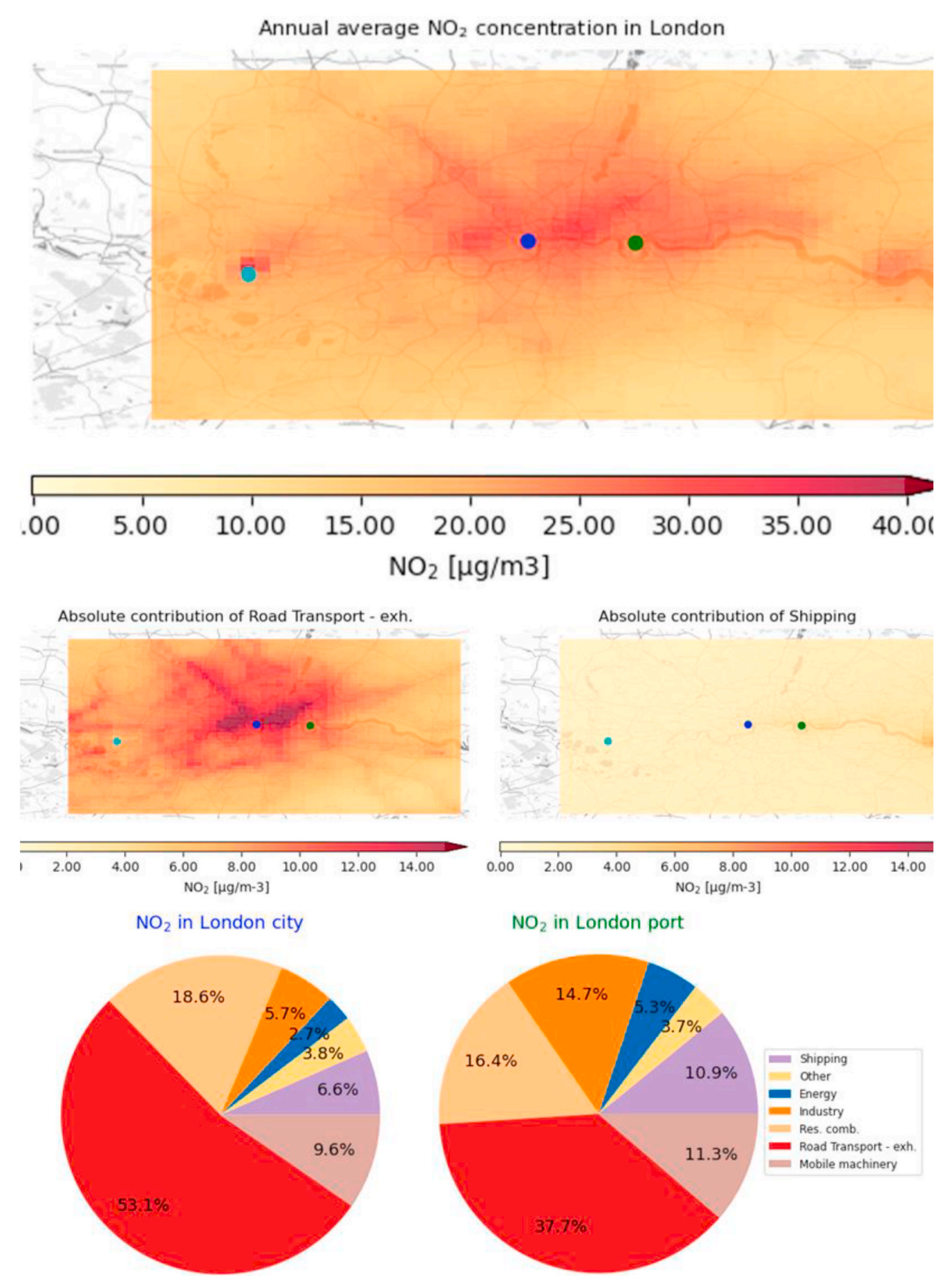


Fig. 11. The modelled annual average  $NO_2$  concentration in and around London (top panel) and the absolute contributions of road transport (exhaust) and shipping to this concentration in respectively the middle left and right panel. The bottom panel shows the contribution from various sectors to the concentration in the city centre (the blue dot at the location of the Big Ben) (left) and at the main container terminal in the port (green dot) (right). Results are for the  $1 \times 1$  km resolution simulation with the TNO GHG-co  $1 \times 1$  km dataset.

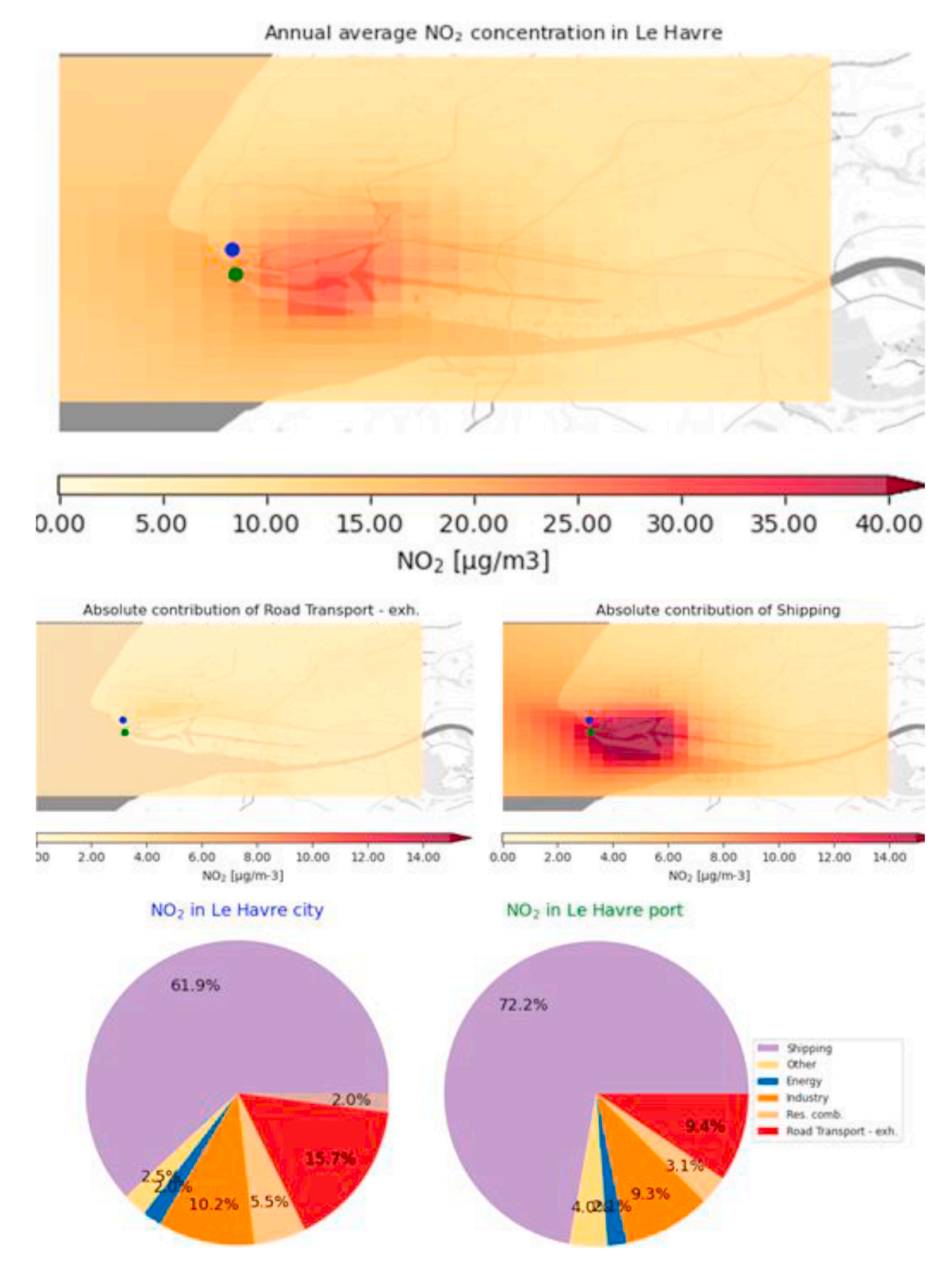


Fig. 12. The modelled annual average  $NO_2$  concentration in and around Le Havre (top panel) and the absolute contributions of the two largest contributors, i.e., road transport (exhaust) and shipping to this concentration in respectively the middle left and right panel. The bottom panel shows the contribution from various sectors to the concentration in the city centre (blue dot at the location of l'Hôtel de Ville) (left) and at the main container terminal in the port (the green dot) (right). Results are for the  $1 \times 1$  km resolution simulation with the TNO GHG-co  $1 \times 1$  km dataset.

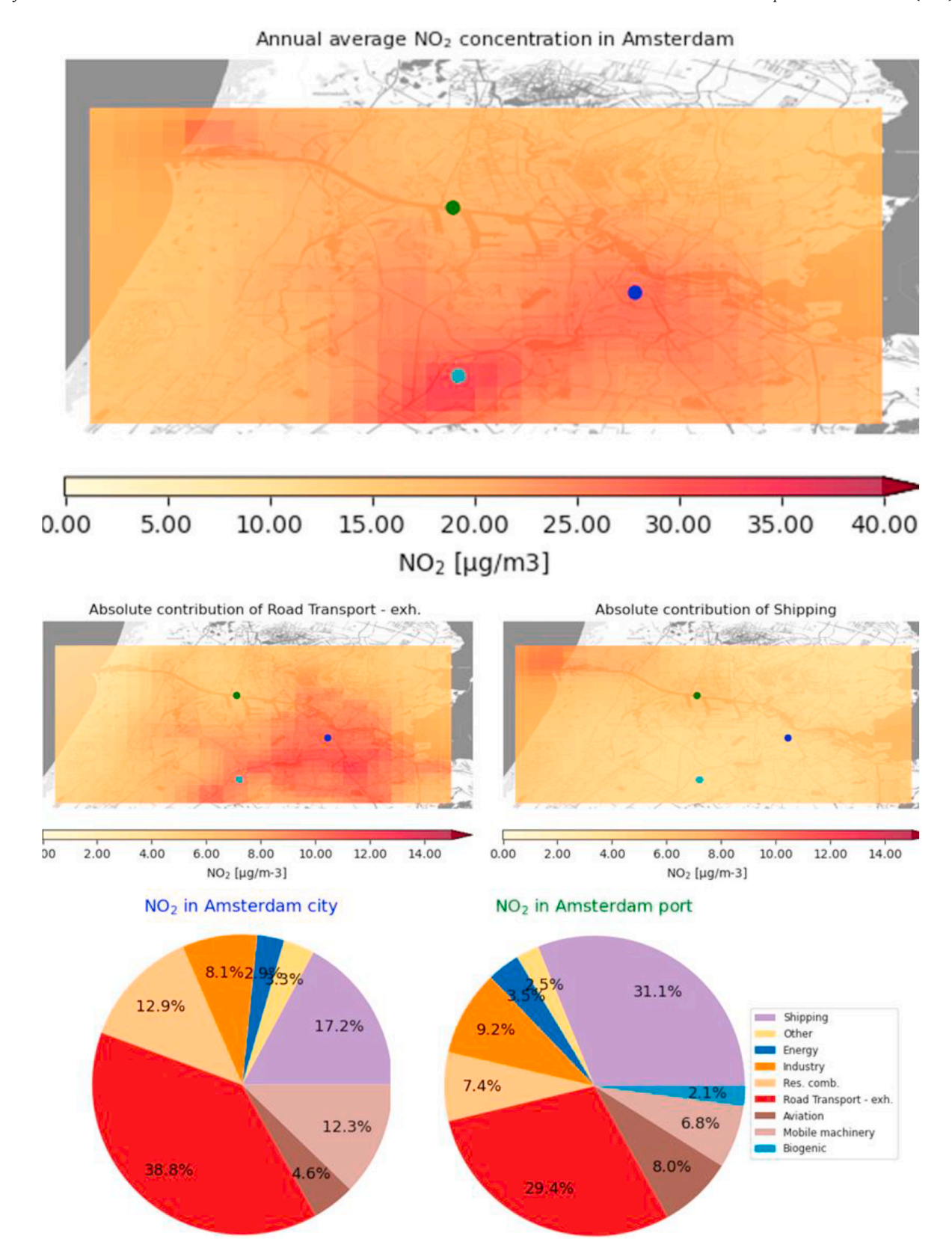


Fig. 13. The modelled annual average  $NO_2$  concentration in and around Amsterdam (top panel) and the absolute contributions of road transport (exhaust) and shipping to this concentration in respectively the middle left and right panel. The bottom panel shows the contribution from various sectors to the concentration in the city centre (the blue dot at the Dam Square) (left) and at the main container terminal in the port (the green dot) (right). Results are for the  $1 \times 1$  km resolution simulation with the ER dataset.

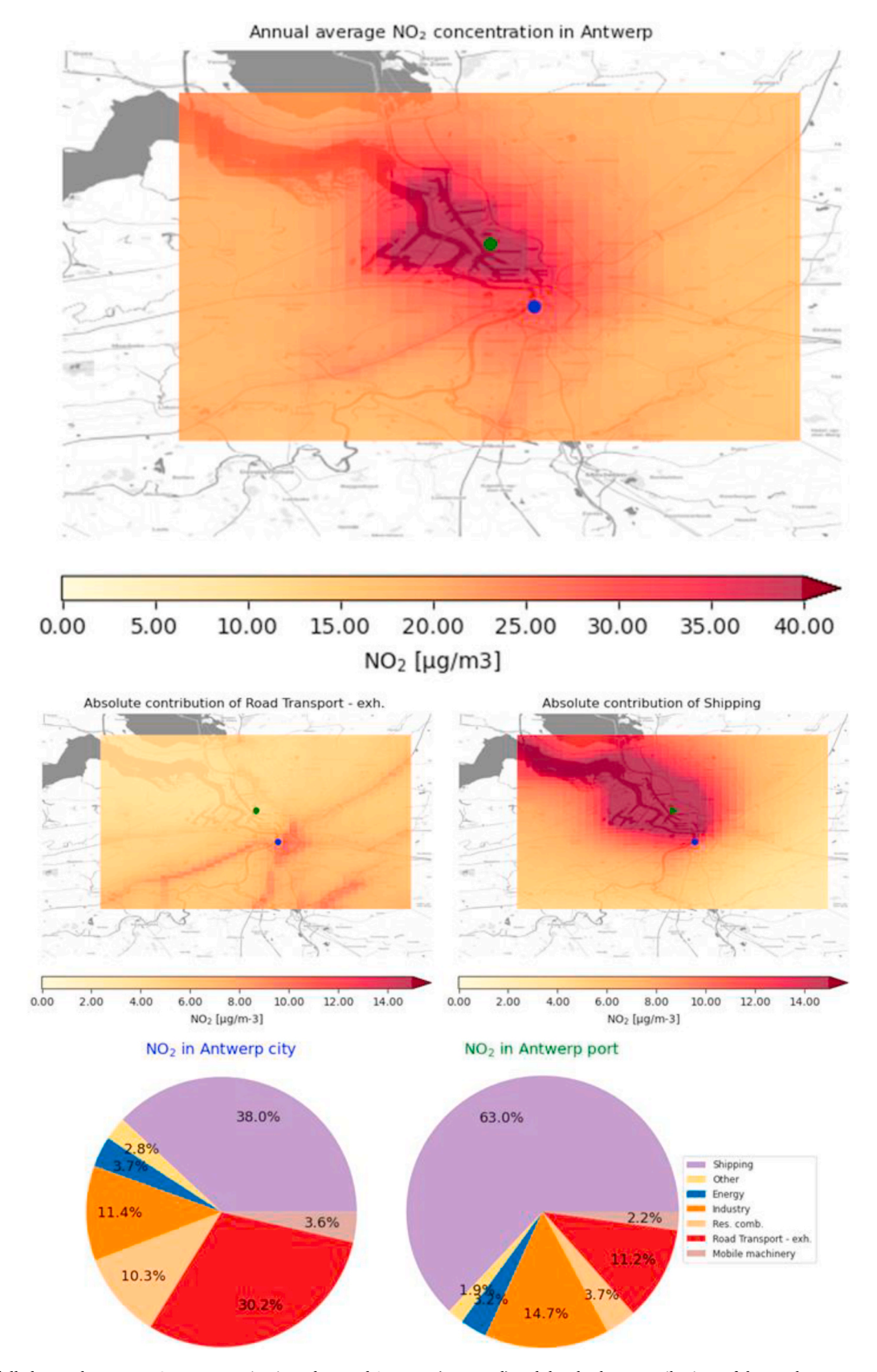
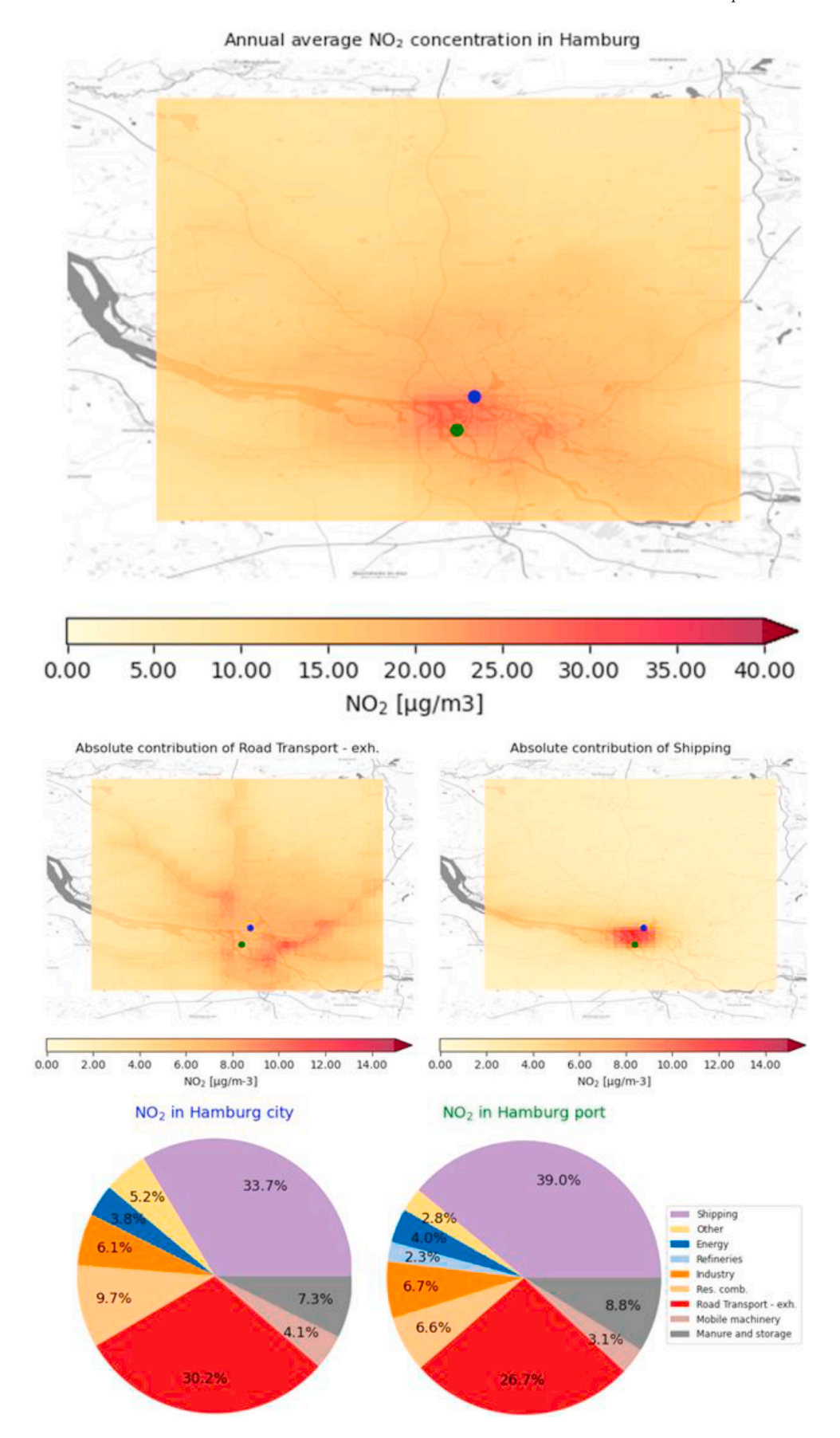


Fig. 14. The modelled annual average  $NO_2$  concentration in and around Antwerp (top panel) and the absolute contributions of the two largest contributors, i.e., road transport (exhaust) and = shipping to this concentration in respectively the middle left and right panel. The bottom panel shows the contribution from various sectors to the concentration in the city centre (the blue dot at the location of the Onze-Lieve-Vrouwekathedraal) (left) and at the main container terminal in the port (the green dot) (right). Results are for the  $1 \times 1$  km resolution simulation with the TNO GHG-co  $1 \times 1$  km dataset.



(caption on next page)

Fig. 15. The modelled annual average  $NO_2$  concentration in and around Hamburg (top panel) and the absolute contributions of the two largest contributors, i.e., road transport (exhaust) and shipping to this concentration in respectively the middle left and right panel. The bottom panel shows the contribution from various sectors to the concentration in the city centre (the blue dot at location of the Hauptkirche Sankt Michaelis) (left) and at the main container terminal in the port (the green dot) (right). Results are for the  $1 \times 1$  km resolution simulation with the GrETA dataset.

#### References

- Alanen, J., et al., 2020. Physical characteristics of particle emissions from a Medium speed ship engine fueled with natural gas and low-sulfur liquid fuels. Environ. Sci. Technol. 54 (9), 5376–5384. https://doi.org/10.1021/acs.est.9b06460.
- Beltman, J.B., et al., 2013. The impact of large scale biomass production on ozone air pollution in Europe. Atmos. Environ. 71, 352–363. https://doi.org/10.1016/j. atmosenv.2013.02.019.
- Bessagnet, B., et al., 2016. Presentation of the EURODELTA III intercomparison exercise evaluation of the chemistry transport models' performance on criteria pollutants and jointanalysis with meteorology. Atmos. Chem. Phys. 16 (19), 12667–12701. https://doi.org/10.5194/acp-16-12667-2016.
- Bieser, J., Aulinger, A., Matthias, V., Quante, M., Denier van der Gon, H.A.C., 2011. Vertical emission profiles for Europe based on plume rise calculations. Environ. Pollut. 159 (10), 2935–2946. https://doi.org/10.1016/j.envpol.2011.04.030.
- Brandt, J., et al., 2013. Assessment of past, present and future health-cost externalities of air pollution in Europe and the contribution from international ship traffic using the EVA model system. preprint. Gases/Atmospheric Modelling/Troposphere/Chemistry (chemical composition and reactions). https://doi.org/10.5194/acpd-13-5923-2013
- Broome, R.A., et al., 2020. The mortality effect of PM2.5 sources in the greater metropolitan region of sydney, Australia. Environ. Int. 137, 105429 https://doi.org/ 10.1016/j.envint.2019.105429.
- Colette, A., et al., 2017. EURODELTA-Trends, a multi-model experiment of air quality hindcast in Europe over 1990–2010. Geosci. Model Dev. (GMD) 10 (9), 3255–3276. https://doi.org/10.5194/gmd-10-3255-2017.
- Concawe, 2023a. The impact of shipping emissions to urban air quality in Europe detailed port-city analysis. report no. 2/23. https://www.concawe.eu/wp-content/uploads/Rpt 23-2.pdf.
- Concawe, 2023b. The impact of aviation emissions to urban air quality in Europe Detailed airport-city analysis. Concawe Report no. 10/23. https://www.concawe.eu/publication/the-impact-of-aviation emissions-to-urban-air-quality-in-europe-detailed-airport-city-analysis/.
- Contini, D., Merico, E., 2021. Recent advances in studying air quality and health effects of shipping emissions. Atmosphere 12 (1), 92. https://doi.org/10.3390/ atmos12010092.
- Denier van der Gon, H.A.C., et al., 2021. VERIFY Observation-Based System for Monitoring and Verification of Greenhouse Gases: Final High Resolution Emission Data 2005-2018 D2.3, D2.3 (TNO GHGco Emission Inventory v3.0).
- Fink, L., Karl, M., Matthias, V., Oppo, S., Kranenburg, R., Kuenen, J., Jutterström, S., et al., 2023a. A multimodel evaluation of the potential impact of shipping on particle species in the Mediterranean Sea. preprint. Aerosols/Atmospheric Modelling and Data Analysis/Troposphere/Chemistry (chemical composition and reactions). https://doi.org/10.5194/egusphere-2023-406.
- Fink, L., Karl, M., Matthias, V., Oppo, S., Kranenburg, R., Kuenen, J., Moldanova, J., et al., 2023b. Potential impact of shipping on air pollution in the Mediterranean region a multimodel evaluation: comparison of photooxidants NO <sub>2</sub> and O <sub>3</sub>. Atmos. Chem. Phys. 23 (3), 1825–1862. https://doi.org/10.5194/acp-23-1825-2022
- Golbazi, M., Archer, C., 2023. Impacts of maritime shipping on air pollution along the US East Coast. Atmos. Chem. Phys. 23 (23), 15057–15075. https://doi.org/10.5194/ acp-23-15057-2023.
- Granier, C., et al., 2019. 'The Copernicus atmosphere monitoring Service global and regional emissions (April 2019 version)'. https://doi.org/10.24380/D0BN-KX16.
- Hersbach, H., et al., 2020. The ERA5 global reanalysis. Q. J. R. Meteorol. Soc. 146 (730), 1999–2049. https://doi.org/10.1002/qj.3803.
- Howard, V., 2009. Statement of evidence particulate emissions and health proposed ringaskiddy waste-to-energy facility. Proposed Ringaskiddy Waste-to-Energy Facility 2011 (4), 1–38.

- Jägerbrand, A.K., et al., 2019. A review on the environmental impacts of shipping on aquatic and nearshore ecosystems. Sci. Total Environ. 695, 133637 https://doi.org/ 10.1016/j.scitotenv.2019.133637.
- Jalkanen, J., Johansson, L., Kukkonen, J., 2016. A comprehensive inventory of ship traffic exhaust emissions in the European sea areas in 2011, 71–84. https://doi.org/1 0.5194/acp-16-71-2016.
- Karl, M., et al., 2019a. Effects of ship emissions on air quality in the Baltic Sea region simulated with three different chemistry transport models. Atmos. Chem. Phys. 19 (10), 7019–7053. https://doi.org/10.5194/acp-19-7019-2019.
- Karl, M., et al., 2019b. Effects of ship emissions on air quality in the Baltic Sea region simulated with three different chemistry transport models. Atmos. Chem. Phys. 19 (10), 7019–7053. https://doi.org/10.5194/acp-19-7019-2019.
- Kranenburg, R., et al., 2013. Source apportionment using LOTOS-EUROS: module description and evaluation. Geosci. Model Dev. (GMD) 6 (3), 721–733. https://doi. org/10.5194/gmd-6-721-2013.
- Kuenen, J., et al., 2022. CAMS-REG-v4: a state-of-the-art high-resolution European emission inventory for air quality modelling. Earth Syst. Sci. Data 14 (2), 491–515. https://doi.org/10.5194/essd-14-491-2022.
- Kuittinen, N., et al., 2021. Shipping remains a globally significant source of anthropogenic PN emissions even after 2020 sulfur regulation. Environ. Sci. Technol. 55 (1), 129–138. https://doi.org/10.1021/acs.est.0c03627.
- Lv, Z., et al., 2018. Impacts of shipping emissions on PM<sub>2.5</sub> pollution in China. Atmos. Chem. Phys. 18 (21), 15811–15824. https://doi.org/10.5194/acp-18-15811-2018.
- Manders, A.M.M., et al., 2017. Curriculum vitae of the LOTOS-EUROS (v2.0) chemistry transport model. Geosci. Model Dev. (GMD) 10 (11), 4145–4173. https://doi.org/ 10.5194/gmd-10-4145-2017.
- Mårtensson, E.M., et al., 2003. Laboratory simulations and parameterization of the primary marine aerosol production: the primary marine aerosol source. J. Geophys. Res. Atmos. 108 (D9), n/a. https://doi.org/10.1029/2002JD002263 n/a.
- Matthias, V., et al., 2010. The contribution of ship emissions to air pollution in the North Sea regions. Environ. Pollut. 158 (6), 2241–2250. https://doi.org/10.1016/j.envpol.2010.02.013
- Monahan, E.C., O'Muircheartaigh, I.G., 1986. Whitecaps and the passive remote sensing of the ocean surface. Int. J. Rem. Sens. 7 (5), 627–642. https://doi.org/10.1080/ 0.143118660096716
- Novak, J.H., Pierce, T.E., 1993. Natural emissions of oxidant precursors. Water, Air, Soil Pollut. 67 (1–2), 57–77. https://doi.org/10.1007/BF00480814.
- Ramacher, M.O.P., et al., 2020. Contributions of traffic and shipping emissions to city-scale NOx and PM2.5 exposure in Hamburg. Atmos. Environ. 237, 117674 https://doi.org/10.1016/j.atmoseny.2020.117674.
- Rémy, S., et al., 2022. Description and evaluation of the tropospheric aerosol scheme in the Integrated Forecasting System (IFS-AER, cycle 47R1) of ECMWF. Geosci. Model Dev. (GMD) 15 (12), 4881–4912. https://doi.org/10.5194/gmd-15-4881-2022.
- Schaap, M., et al., 2008. The LOTOS EUROS model: description, validation and latest developments. Int. J. Environ. Pollut. 32 (2), 270. https://doi.org/10.1504/ LIEP.2008.017106.
- Schneider, C., et al., 2016. ArcGIS basierte Lösung zur detaillierten, deutschlandweiten Verteilung (Gridding) nationaler Emissionsjahreswerte auf Basis des Inventars zur Emissionsberichterstattung (TEXTE 71.
- Tang, L., et al., 2020. The impact of ship emissions on air quality and human health in the Gothenburg area Part 1: 2012 emissions. Atmos. Chem. Phys. 20 (12), 7509–7530. https://doi.org/10.5194/acp-20-7509-2020.
- Timmermans, R., et al., 2022. Evaluation of modelled LOTOS-EUROS with observational based PM10 source attribution. Atmos. Environ. X 14, 100173. https://doi.org/10.1016/j.aeaoa.2022.100173.
- Visschedijk, A., Denier van der Gon, H., 2022. UFP emissie in de Rijnmond regio in 2019', DCMR Milieudienst Rijnmond. TNO, 2022 R(060.49283).
- Wever, D., et al., 2021. Informative Inventory Report 2021. Emissions of transboundary air pollutants in The Netherlands 1990–2019. Rijksinstituut voor Volksgezondheid en Milieu. https://doi.org/10.21945/RIVM-2021-0005.